List of Publications

1. Redox polymerization of acrylamide to high molecular weights: effect of the mineral clay montmorillonite.
   P.Bera and S. K. Saha, *Macromol. Rapid Commun.*, **18**, 261-265 (1997).
   (Based on the works incorporated in chapter 3, section 3.3 and 3.4)

2. Redox polymerization of acrylamide on aqueous montmorillonite surface: Kinetics and mechanism of enhanced chain growth.
   P. Bera and S. K. Saha, *Polymer*, **39**, 1461-1469 (1998).
   (Based on the works incorporated in chapter 3, section 3.4)

3. Selective trapping of the initiator component in the interlayer space of montmorillonite: A novel technique of controlling linear termination in aqueous acrylamide polkymerization.
   P. Bera and S. K. Saha, *Ind. J. Chem. Tech.*, **6**, 24-30 (1999).
   (Based on the works incorporated in chapter 3, section 3.3)

4. Water-soluble copolymers of acrylamide with diacetone acrylamide and N-t-butylacrylamide on aqueous montmorillonite surface: Synthesis and characterisation.
   P. Bera and S. K. Saha, *Eur. Polym. J.*, December, (1999) (in Press).
   (Based on the works incorporated in chapter 4)

5. Molecular dimension and interaction parameters of polyacrylamide in water-dimethylsulphoxide mixtures: Effect of temperature.
   P. Bera and S. K. Saha, *Eur. Polym. J.*, (communicated)
   (Based on the works incorporated in chapter 5)

6. Solid phase polymerization of acrylamide on montmorillonite surface: Kinetics and mechanism.
   P. Bera and S. K. Saha, *J. Ind. Chem. Soc.*, (communicated)
   (Based on the works in corporated in chapter 3, section 3.5)

Redox polymerization of acrylamide to high molecular weights: effect of the mineral clay montmorillonite

*P. Bera, S. K. Saha**

Department of Chemistry, University of North Bengal,
Raja Rammohunpur, PIN-734430 Dt. Darjeeling, West Bengal, India

(Received: September 25, 1996)

SUMMARY:

Polymerization of acrylamide with the redox couple Fe(III)/thiourea in the presence of the mineral clay montmorillonite has been investigated. Polyacrylamide is obtained in good yield having molecular weight (ca. 0.7 2.5 × 10^6) approximately one order of magnitude higher than without clay. Apparently, the locus of polymerization is the interlayer space of the clay.

Introduction

In view of the use of polyacrylamide as water soluble viscofier and displacement fluid in secondary oil recovery, hydrodynamic volume and intrinsic viscosity of the polymer are of fundamental importance. Redox-initiated polymerization of acrylamide often yields polymers having not so high molecular weights and intrinsic viscosities because of the fast termination process via transfer to the oxidant (viz., metal ions at higher oxidation state) of the initiating redox couple[1]. In this communication we report a method of preparing comparatively higher molecular weight polymers of acrylamide with higher intrinsic viscosity, initiated by ferric ion/thiourea (TU) redox couple in presence of montmorillonite. Montmorillonite is a 2:1 type of trimorphic layered phyllosilicate (smectite) in which the central octahedral aluminium is surrounded by two tetrahedral silica sheets[2]. It has strong sorptive properties due to the expandibility of the mineral layers and has been shown to catalyze the polymerization of some unsaturated organic compounds such as styrene and hydroxyethyl methacrylate but yet to inhibit polymer formation from other structurally related monomers such as methyl methacrylate[3]. This behaviour is believed to be due to the electron-accepting or electron-donating sites on the clay minerals. In order to check the linear termination process and to increase the degree of polymerization, we loaded the Fe(III) ions in the interlayer spaces of the mineral and successfully prepared polymers of acrylamide in presence of TU. For the purpose of comparison, same experiments were conducted with Fe(III)/TU redox initiator in absence of the mineral.

Experimental part

Acrylamide (AM, reagent grade, Fluka) and thiourea (TU, Merck) were purified as usual. Montmorrilonite (diameter <2 μm) was purified following methods described elsewhere[2,3]. Fe(III) ions were loaded onto the exchangeable sites of montmorillonite

 CCC 1022-1336/97/$02.50

(Fe(III)) up to maximum saturation (0.9 meq · g^{-1}) by shaking a known amount of the mineral with $FeCl_3$ solution for 5 h, followed by repeated centrifugation (20000 rpm) and washing with double distilled water. Polymerization reactions were carried out in aqueous solution under pure nitrogen in absence of light. Intrinsic viscosities were measured by Ubbelohde viscometer with water flow rate of 2 mL · s^{-1} at 30 °C, and the molecular weights were calculated using the Mark-Houwink relationship[4]:

$$[\eta] = 9.33 \times 10^{-3} \bar{M}^{0.75} \text{ (mL} \cdot \text{g}^{-1}\text{)}$$

Results and discussion

Tab. 1 shows the data pertaining to the initial rates of polymerization (R_p), polymer yields (X_L), intrinsic viscosities ([η]) and molecular weights ($\bar{M}_v$) of the polymers formed as functions of the concentration of Fe(III) ions, TU and monomer concentrations, pH and temperature, in the presence as well as in absence of montmorillonite. In homogeneous reaction conditions (i.e., in absence of clay mineral), R_p decreases with Fe(III) ion concentration, which is consistent with previous reports on similar redox systems and supports linear termination hypothesis by the metal ion[1,5–8]. The rate dependence on the monomer concentration could neither be related to a first-order nor a second-order reaction, and the slope of the R_p vs. [AM] plot is found to be 1.45. Referring to the literature concerned with other redox systems involving metals as oxidants, the above kinetic behaviour supports a similar polymerization mechanism as reported earlier[7]. At low concentration of TU, a first-order reaction with respect to TU is observed. On the other hand, R_p, polymer yield and polymerization mechanism are influenced to a great extent when Fe(III) ions were trapped in the interlayer spaces of montmorillonite. R_p increases linearly with Fe(III) ion concentration, with an exponent of 0.25 and 0.40 at temperatures of 50 and 70 °C, respectively, while the rate dependence on TU concentration remains the same. An appreciable "gel effect" is observed, apparently due to slower termination rates in presence of the mineral[9]. The initial rate of polymerization also increases with increasing monomer concentration. The corresponding monomer exponent is 2.3. Such a high monomer exponent is striking but not totally unusual and may be attributed to the "cage effect" where the montmorillonite microenvironment forms a potential barrier which prevents the initiating TU radicals to diffuse immediately, thus favouring their destruction by mutual recombination[10].

Above all, the polymers formed have much higher intrinsic viscosity and molecular weight than those observed in absence of montmorillonite. The [η] values of polymers formed in homogeneous solution (absence of montmorillonite) varied from 14 to 108 mL · g^{-1} (Tab. 1) under the present experimental conditions. Previous reports show that redox polymerization always displayed low intrinsic viscosities and molecular weights. Tab. 1 records highest values of [η] and $\bar{M}_v$ from each of the references. On the other hand, [η] values of polymers formed in presence of montmorillonite are found to vary from 208 to 595 mL · g^{-1} under identical experimental conditions. The [η] values also increase with increasing monomer and TU concen-

Tab. 1. Results of acrylamide (AM) polymerization with the redox couple Fe(III)/thiourea (TU) in presence and absence of montmorillonite (MO)

[Fe(III)] [a] mmol · L^{-1}	[MO] in %	[TU] mol · L^{-1}	[AM] mol · L^{-1}	pH	Temp. in °C	$R_p \times 10^3$ [b]	X_L [c] in %	$[\eta]$ [d] mL · g^{-1}	$\bar{M}_v \times 10^{-5}$
0.60	0.2	0.04	0.4	2.01	50	2.86	61	340	12.0
0.90	0.3	0.04	0.4	2.01	50	3.33	62	364	12.2
1.50	0.5	0.04	0.4	2.00	50	2.64	76	369	12.5
2.07	0.7	0.04	0.4	2.01	50	3.97	77	284	9.5
2.67	0.9	0.04	0.4	2.01	50	3.90	60	291	9.8
1.5	0.5	0.01	0.4	2.00	50	1.04	42	487	19.5
1.5	0.5	0.02	0.4	2.02	50	2.56	50	595	25.0
1.5	0.5	0.03	0.4	2.01	50	2.60	55	560	23.0
1.5	0.5	0.04	0.3	2.01	50	1.08	63	363	12.2
1.5	0.5	0.04	0.5	2.01	50	3.60	48	397	14.9
1.5	0.5	0.04	0.6	2.01	50	5.56	57	480	19.1
1.5	0.5	0.04	0.4	2.01	45	1.02	66	208	6.2
1.5	0.5	0.04	0.4	2.01	60	3.72	84	432	16.6
1.5	0.5	0.04	0.4	2.00	70	3.98	94	220	6.8
1.5	0.5	0.04	0.4	1.52	50	2.65	63	300	10.0
1.5	0.5	0.04	0.4	2.10	50	3.09	40	369	12.5
1.5	0.5	0.04	0.4	2.87	50	–	–	–	–

Tab. I. Continued

[Fe(III)] [a] mmol · L^{-1}	[MO] in %	[TU] mol · L^{-1}	[AM] mol · L^{-1}	pH	Temp. in °C	$R_p \times 10^3$ [b]	X_1 [c] in %	$[\eta]$ [d] mL · g^{-1}	$\bar{M}_v \times 10^{-5}$
1.5[e]	–	0.04	0.4	2.00	50	4.40	73	64	1.3
3.0[e]	–	0.04	0.4	2.01	50	5.60	56	73	1.5
4.0[e]	–	0.04	0.4	2.01	50	1.02	40	41	0.7
8.0[e]	–	0.04	0.4	2.01	50	2.50	26	45	0.8
1.5[e]	–	0.04	0.3	2.01	50	5.00	62	60	1.2
1.5[e]	–	0.04	0.6	2.01	50	13.00	77	108	2.6
1.5[e]	–	0.01	0.4	2.00	50	1.78	40	14	0.2
Ce(IV)/TU (ref.[5])									0.9
Mn(III)/EAA (ref.[6])								0.5	0.2
Ce(IV)/EDTA (ref.[7])								133	1.8
Ce(IV)/NTA (ref.[8])								90	1.1
Ce(IV)/NPA (ref.[1])								68	0.8
Ce(IV)/IDA (ref.[1])								73	0.9

[a] Interlayer Fe(III).
[b] Initial rate in mol · L^{-1} · s^{-1}.
[c] Yield after 4.5 h.
[d] Intrinsic viscosity.
[e] Fe(III) in solution.

trations, and increase with temperature up to 50 °C and then tend to decrease at higher temperatures. The $\overline{M}_v$ values as calculated from the viscosity data ranged from 0.7×10^6 to 2.5×10^6. Comparison of $\overline{M}_v$ with literature values is to be done carefully because previous workers used a different Mark-Houwink relation.

XRD studies showed that basal spacing of the present montmorillonite sample is 14 Å, and all the species, viz., Fe(III) ions, TU and monomers, are intercalated between the layers of the mineral without expanding the same. Polymerization increases basal spacing up to 15 Å, and glycerol treatment does not have any effect at this stage. It seems apparent that the locus of the polymerization reaction is the interlayer space of the mineral, and the position of Fe(III) ions eventually retards the linear termination process, resulting in the high degree of polymerization. ^{13}C NMR spectra confirm head-to-tail polymers with mixed tacticities in which Bernoulli statistics is followed[11].

Acknowledgement: The authors are thankful to the *C.S.I.R.*, New Delhi, for financial support.

[1] W. C. Hsu, J. F. Kuo, C. Y. Chen, *J. Polym. Sci., Part A: Polym. Chem.* **31**, 267 (1993)
[2] J. Bhattacharya, S. K. Chakravarti, S. Talapatra, S. K. Saha, S. C. Guhaniyogi, *J. Polym. Sci., Part A: Polym. Chem.* **27**, 3977 (1989)
[3] J. Bhattacharya, S. K. Saha, S. C. Guhaniyogi, *J. Polym. Sci., Part A: Polym. Chem.* **28**, 2249 (1990)
[4] J. Francois, D. Sarazin, T. Schwartz, G. Weill, *Polymer* **20**, 969 (1979)
[5] G. S. Misra, S. N. Bhattacharya, *J. Polym. Sci., Polym. Chem. Ed.* **20**, 131 (1982)
[6] T. Balakrishnan, S. Subbu, *J. Polym. Sci., Part A: Polym. Chem.* **24**, 2271 (1986)
[7] W. C. Hsu, J. F. Kuo, C. Y. Chen, *J. Polym. Sci., Part A: Polym. Chem.* **30**, 2459 (1992)
[8] W. C. Hsu, C. Y. Chen, J. F. Kuo, E. M. Wu, *Polymer* **35**, 849 (1994)
[9] J. E. McGrath, *J. Chem. Edu.* **58**, 844 (1981)
[10] J. P. Riggs, F. Rodriguez, *J. Polym. Sci., Part A-1* **5**, 3151 (1967)
[11] J. E. Lancaster, M. N. O'Connor, *J. Polym. Sci., Polym. Lett. Ed.* **20**, 547 (1982)

Polymer Vol. 39 Nos. 6–7, pp. 1461–1469, 1998

0032-3861/97/$17.00+0.00

PII: S0032-3861(97)00359-5

Redox polymerisation of acrylamide on aqueous montmorillonite surface: kinetics and mechanism of enhanced chain growth

P. Bera and S. K. Saha*
Department of Chemistry, University of North Bengal, Darjeeling 734430, India
(Received 15 August 1996; revised 25 March 1997)

Aqueous polymerisation of acrylamide by Fe(III)–thiourea redox couple has been studied in homogeneous conditions as well as by loading Fe(III) ions in the interlayer spaces of montmorillonite. A dramatic effect was observed in the latter case, resulting in a very high degree of polymerisation and yielding polymers having high intrinsic viscosity due to imposed constraint on linear termination process. The technique, in general, demonstrates a promising method of achieving high molecular weight polymers by redox initiators. Polymerisation locus was identified and propagating radicals were characterised by XRD and e.s.r., respectively. The polymers were characterised by ^{1}H and ^{13}C n.m.r. spectroscopy. Kinetics of the polymerisation reaction is investigated and the mechanism of the reaction is discussed. © 1997 Elsevier Science Ltd. All rights reserved.

(Keywords: aqueous polymerisation; acrylamide; montmorillonite)

INTRODUCTION

Ability of clay minerals to intercalate various molecules and their catalytic properties are long known. The clay–polymer interaction has found many and varied applications[1]. Interest in clay–polymer combinations stems from the use of clay minerals as fillers and reinforcers in polymer systems. All things being equal, the efficiency of a filler in improving the physico-chemical properties of a polymer system is primarily determined by the degree of its dispersion in the polymer matrix. The most effective way of achieving such compatibility is to graft a suitable polymer on to filler surface and/or to encapsulate the mineral particles with the former by polymerising monomers directly on filler surfaces[2]. Montmorillonite, a smectite clay has been shown to catalyse the polymerisation of some unsaturated organic compounds such as styrene and hydroxy ethyl methacrylate and yet to inhibit polymer formation from other structurally related monomers such as methyl methacrylate[3]. This behaviour is believed to be due to the electron accepting or electron donating sites on the clay minerals. However, it has been shown recently that montmorillonite can be used in conjunction with organic substances, viz., alchols, thioureas, etc. to polymerise methyl methacrylate in aqueous medium[3,4].

In view of increasing industrial applications of water soluble acrylamide polymers, clay minerals and their combinations in various fields including the use of polyacrylamide as water soluble viscofier in enhanced oil recovery, we undertake the present study with two major objectives: (i) to examine the catalytic activity of montmorillonite on the polymerisation of acrylamide in aqueous medium and, (ii) to prepare acrylamide polymer having large hydrodynamic volume and molecular weights by Fe(III)/thiourea redox initiator in presence of montmorillonite.

*To whom correspondence should be addressed

EXPERIMENTAL

Materials

Acrylamide (AM, reagent grade, Fluka) was purified by recrystallisation from methanol (two times) and dried in vacuum oven at 45°C overnight. Thiourea (TU, E.Merck) was used after recrystallisation three times from distilled water (m.p. 180°C). A suspension of montmorillonite (Mo) having particle size less than 2 μm (diameter) was prepared by sedimentation[3]. Free iron oxides were removed by dithionite–citrate method. Organic matters were removed following method described elsewhere[5]. H^+-montmorillonite (HM) was prepared by shaking the stock of the mineral (3% w/v) in presence of 0.5 M HCl for about 6 h followed by repeated centrifugation (20 000 rpm) and washing with double distilled water. The cation exchange capacity (CEC) of montmorillonite was determined by potentiometric titrations with standard KOH solution under nitrogen atmosphere and was found to be 0.91 meq g^{-1}. Fe(III)-montmorillonite (FeM) was prepared by shaking HM suspension (3% w/v) in presence of 0.5 M $FeCl_3$ (reagent grade) at pH 2.5 for 6 h followed by purification by repeated centrifugation and washing with distilled water until the test of Fe(III) ions in the supernatent was negative. A separate experiment on the sorption of Fe(III) on to montmorillonite shows that the maximum intake of Fe(III) ions by HM samples slightly exceeds the CEC value viz., 0.98 meq g^{-1}.

Polymerisation

Measured quantities of aqueous solutions of AM were added to known amounts of HM or FeM suspension or their various mixtures in well stoppered pyrex bottles under nitrogen atmosphere and were equilibrated at required temperature. Deaerated TU solutions were then added to these solutions and the reactions were allowed to continue for desired time span in absence of any light. Polymerisation reactions were stopped by diluting the mixture with chilled

water keeping the reaction vessels in ice bath. The mixtures were then centrifuged to remove HM/FeM. The polyacrylamide (PAM) was precipitated out by adding excess of acetone, washed repeatedly with acetone and dried in vacuum at 40°C for 48 hours. Molecular weights of the polymer were determined by viscosity measurement in aqueous 0.1 M NaCl solution using a Ubbelohde viscometer and a Mark–Houwink relationship of the type[6,7]:

$$[\eta] = 9.33 \times 10^{-3} \bar{M}^{0.75} \text{ cm}^3/\text{g}$$

E.s.r., n.m.r. and XRD measurements

E.s.r. spectra were recorded at room temperature with a Varian V4502 spectrometer using 100 kHz magnetic field modulation. Instrumental setup and technique were the same as described previously[8]. ^{1}H and ^{13}C n.m.r. spectra were recorded on a Varian XL-300 spectrometer in D_2O. Chemical shifts were measured with reference to dioxane at $\delta = 67.40$ ppm. The X-ray powder diffraction patterns of solid minerals were recorded with a Philips PW 1730 machine using Ni-filtered CuK_α radiation. X-ray generator was operated at 40 kV/20 mA.

RESULTS AND DISCUSSION

Montmorillonite possesses a layered structure and has strong sorptive properties due to expandability of the mineral layers. It is a 2:1 type or trimorphic layered phyllosilicate in which the central octahedral aluminium is surrounded by two tetrahedral silica sheets. Substitution by Fe^{2+}, Fe^{3+} or Mg^{2+} normally occurs in the octahedral position of aluminium. The isomorphous replacement of both bi and trivalent metals from the lattice position to the mineral surface may also take place slowly on standing. The mineral can accept electrons via the aluminium at the crystal edges and the transition metals, such as Fe(III), in the silicate layers. Aluminium in octahedral coordination acts as a Lewis acid if its coordination water molecules are removed by drying. On the other hand, the electron donor sites are transition metals in the reduced state. Iron in the crystal lattice of montmorillonite participates in various chemical reactions in the layered spaces. One of the examples is the well known reaction of montmorillonite with benzidine molecule to form benzidine blue in which the lattice substituted Fe(III) ions are involved[9].

Montmorillonite especially, and other clay minerals in general, give powder e.s.r. spectra containing a multiplicity of lines, which essentially fall into three zones. *Figure 1a* shows e.s.r. spectra of the present montmorillonite sample containing 0.03% and 2.14% (w/w with respect to mineral wt.) iron in exchangeable and lattice positons respectively. Signal near $g = 4.3$ due to paramagnetic Fe^{3+} cations may be attributed to cis and trans octahedral sites, having axial and rhombic symmetry. A very broad signal near $g = 2.2$ arises from exchange interactions between clusters of Fe^{3+} ions which may be present on the surfaces of the smectite as well as due to hydrated Fe^{3+} in the exchangeable sites[10]. A very small but sharp signal at $g = 2.00$ has been assigned to structural defects. *Figure 1b* shows the e.s.r. spectrum that arises from the same montmorillonite sample but pretreated with excess of TU at 50°C for 30 min under nitrogen. Significant decrease of the intensity at $g = 4.3$ signal indicates that TU reacts with lattice Fe(III) and forms non-Kramers species which are e.s.r. silent. Bhattacharya and coworkers put forward chemical and electrochemical evidences to show that isothiocarbamido radicals (I)

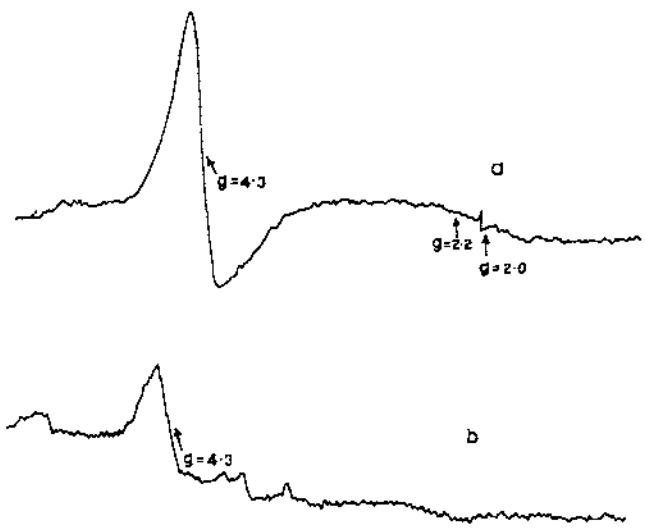

Figure 1 E.s.r. spectra of air dried powder montmorillonite sample at 20°C: (a) H^+ exchanged; (b) pretreated with thiourea at 50°C under N_2

formed in above reaction can activate radical polymerisation of methyl methacrylate in aqueous medium[11].

However, in the present study, attempts to polymerise water soluble acrylamide monomers by lattice-Fe(III)/TU combination were unsuccessful at a wide range of temperature. This is probably due to efficient inhibition of radical polymerisation of acrylamide by montmorillonite via electron transfer from initiating or propagating radicals to the Lewis acid sites. On the other hand, montmorillonite microenvironment seems to have a dramatic effect on the redox polymerisation of acrylamide by Fe(III)–TU combination. In view of the fact that redox initiated polymerisation of acrylamide often yield polymers having not so high molecular weights and intrinsic viscosities primarily because of the fast termination process via transfer to the oxidant (viz., metal ions at higher oxidation state) of the initiating redox couple, we loaded Fe(III) ions in the interlayer spaces of the mineral to control the rate of termination and examined the effect on acrylamide polymerisation in presence of TU[12]. For the purpose of comparison of the results, same experiments were duplicated as controls with Fe(III)/TU redox initiator in absence of the mineral. *Figure 2* shows that the conversion efficiencies are increased dramatically when the Fe(III) ions are loaded in the layered spaces of montmorillonite. Fe(III)/TU redox couple brings about 40% conversion at 45°C (in the absence of any montmorillonite), which is increased slightly with temperature when 4.0×10^{-3} mol l^{-1} $FeCl_3$ is used (TU = 0.04 mol l^{-1}) at pH 2.01. However, 94% conversion is observed for the same concentration of Fe(III) ion when loaded in the interlayer space of montmorillonite ($\overline{Fe}$(III)) under identical conditions (concentration of $\overline{Fe}$(III) being moles of interlayer metal ions per 1000 mL of the reaction mixture). No induction period is observed, however, in either case. At lower $FeCl_3$ concentrations, polymer yield (X_L) as well as the initial rate of reaction (R_p) were increased substantially, indicating slower termination rates in the absence of any mineral clay. On the other hand, in the presence of mineral microenvironment, the initial rate of polymerisation was increased from 2.83×10^{-3} to 3.97×10^{-3} mol l^{-1} min^{-1} as the $\overline{Fe}$(III) concentration increased from 0.60×10^{-3} to 2.07×10^{-3} mol l^{-1}. At a higher concentration of $\overline{Fe}$(III), however, R_p tends to decrease due to transfer to ferric ions. Conversion

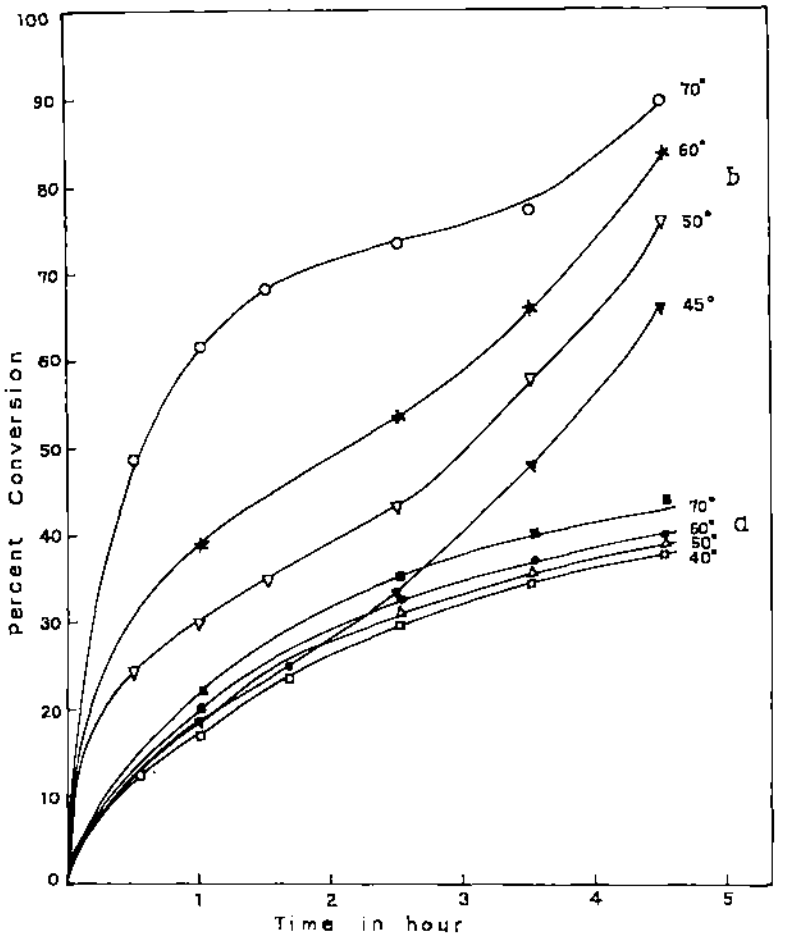

Figure 2 The effect of Fe(III) loading in montmorillonite on the course of polymerisation at various temperatures: (a) [Fe(III)] = 0.004 mol l^{-1}, [Mo] = 0, [TU] = 0.04 mol l^{-1}, [AM] = 0.4 mol l^{-1}, pH 2.01; (b) [Fe(III)] = 0.004 mol l^{-1}, [Mo] = 1.4%, [TU] = 0.04 mol l^{-1}, [AM] = 0.4 mol l^{-1}

efficiencies were also increased regularly with increasing Fe(III) ion concentration up to 2.07×10^{-3} mol l^{-1}. Although R_p and the yield decreased with decreasing TU concentrations, molecular weight of the polymer was higher at lower TU concentrations. Moreover, significant 'gel-effect' was observed in the presence of clay mineral apparently due to decrease in termination rates as mentioned above as well as for comparatively higher viscosity of the medium[13]. 'Gel-effect' was more prominent at lower temparatures than at 70°C. *Table 1* represents the data pertaining to the initial rates of polymerisation (R_p), polymer yeild (X_1), intrinsic viscosity (η) and molecular weight ($\bar{M}_v$) of the polymers formed as functions of the concentration of Fe(III), TU, AM, pH and temperature in the presence as well as in the absence of montmorillonite. The most significant observation of loading Fe(III) ions of the initiating redox couple in the interlayer spaces of montmorillonite is achieving polymers with much higher intrinsic viscosity and molecular weight. The η value of the polymer formed in homogeneous solution and in the absence of the mineral varied from 14 to 90 ml g^{-1} (*Table 1*) under the present experimental condition. Previous reports showed that redox polymerisation always displayed low intrinsic viscosities and molecular weights as are depicted in *Table 2* (which records the highest values of η and $\bar{M}_v$ from each of the References [12,14–17]). On the other hand, η values displayed by polymers formed in presence of montmorillonite were found to vary from 247 to 600 ml g^{-1} under identical experimental conditions. The η is also increased with increasing monomer and TU concentrations while it is increased with temperature up to 50°C but decreased at higher temperatures. The $\bar{M}_v$ values as calculated from viscosity data of present experiments ranged from 0.62×10^6 to 2.5×10^6. However, comparison of $\bar{M}_v$ with literature values should be done carefully because previous workers applied a different Mark–Houwnik equation. The significant role played by montmorillonite probably stems from two factors: (i) polymer initiation in the mineral microenvironment is favoured and (ii) rate of linear termination process decreases significantly because transfer to Fe(III) ions is highly restricted for the latter's location in the layered spaces of the mineral and diffusion of the living radical through montmorillonite gel is rather slow. In general, loading of the oxidant, i.e. metal ions, of the redox couple in the interlayer space of clay minerals, i.e. montmorillonite, offers a potential method of achieving very high degree of polymerisation for a redox initiated reactions.

Generation of primary and propagating free radicals

Previous studies showed that polymerisation of various

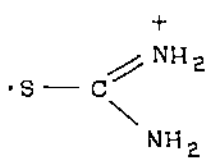

(I)

Table 1 The initial rates of polymerisation, polymer yields, intrinsic viscosities and the molecular weights of Fe(III)–TU initiated polymerisation in the presence and absence of montmorillonite at various conditions

Temp. (°C)	pH	[Mo][a] (g l^{-1})	[$\overline{Fe}$(III)][b] (mmol l^{-1})	[TU] (mol l^{-1})	[AM] (mol l^{-1})	$R_p \times 10^3$ (mol l^{-1} m^{-1})	X_L[c] (%)	η (ml g^{-1})	$\bar{M}_v$ ($\times 10^{-5}$)
		2.0	0.60			2.86	61	340	12.0
		3.0	0.90			3.33	62	364	12.2
50	2.01	5.0	1.50	0.04	0.40	2.64	76	369	12.5
		7.0	2.07			3.97	77	284	9.5
		9.0	2.67			3.90	60	291	9.8
				0.01		1.04	42	487	19.5
50	2.01	5.0	1.50	0.02	0.40	2.56	50	595	25.0
				0.03		2.60	55	560	23.0
					0.30	1.08	63	363	12.2
50	2.01	5.0	1.50	0.04	0.50	3.60	48	397	14.9
					0.60	5.56	57	480	19.1
45						1.02	66	208	6.2
60	2.01	5.0	1.50	0.04	0.40	3.72	84	432	16.6
70						3.98	94	220	6.8
	1.52					2.65	63	300	10.0
50	2.10	5.0	1.50	0.04	0.40	3.09	40	369	12.5
	2.87					–[d]	–	–	–
			0.38 (0.008)			1.23	36	290	9.8
50	2.01	5.0	0.75 (0.015)	0.04	0.40	1.99	43	360	13.0
			1.13 (0.023)			2.22	45	355	12.8
			1.50[e]			4.40	73	64	1.3
50	2.01		3.00[e]	0.04	0.40	5.60	56	73	1.5
			4.00[e]			1.02	40	61	0.7
			8.00[e]			2.50	26	45	0.8
				0.04	0.30	5.0	62	60	1.2
50	2.01		1.5[f]	0.04	0.60	13.00	77	108	2.6
				0.01	0.40	1.78	40	14	0.2

[a]Montmorillonite content
[b]Concentration of interlayer Fe(III) in mmol l^{-1} of the reaction mixture; corresponding concentrations in montmorillonite gel phase is 0.03 mol l^{-1} throughout, except those shown in brackets
[c]Yield after 4.5 hrs. [d]No polymer formed. [e]Concentration of $FeCl_3$ in solution

Figure 3 E.s.r. spectrum of MNP–PAM spin adduct

water insoluble vinyl monomers initiated by redox couples involving TU as the reductant, involved isothiocarbamido primary free radicals (I) in aqueous acid solution[11].

Owing to high 'g' anisotropy and a very short relaxation time, detection of this radical by e.s.r. spectroscopy was not possible until recently, when e.s.r. study of spin adducts of the radical was reported[8]. In the present system also it is believed that the same primary radical (I) is formed and the propagating radicals from acrylamide are trapped by methyl nitroso propane (MNP) spin trap. *Figure 3* shows the e.s.r. spectrum of the MNP spin adduct of the radical (II)

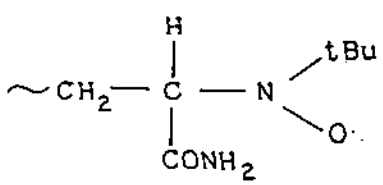

(II)

Table 2 Intrinsic viscosities and molecular weights of acrylamide polymers formed by different redox couples

Initiating system	η (ml g^{-1})	$\bar{M}_v$ ($\times 10^{-5}$)
Ce(IV)–thiourea[14]	–	0.9
Mn(III)–ethoxyacetic acid[15]	0.5	0.2
Ce(IV)–ethylenediamine tetraacetic acid[16]	133	1.8
Ce(IV)–nitrilotriacetic acid[17]	90	1.1
Ce(IV)–nitrilotripropionic acid[12]	68	0.8
Ce(IV)–iminodiacetic acid[12]	73	0.9

The spectrum depicts a 1:1:1 triplet of doublets. The triplet is undoubtedly originated from the nitroxide radical (a_N = 1.45 mT) of MNP and the doublets are generated from H^β splitting (a_H = 0.31 mT). The isothiocarbamido radicals (I) are, however, not trapped by MNP under present condition.

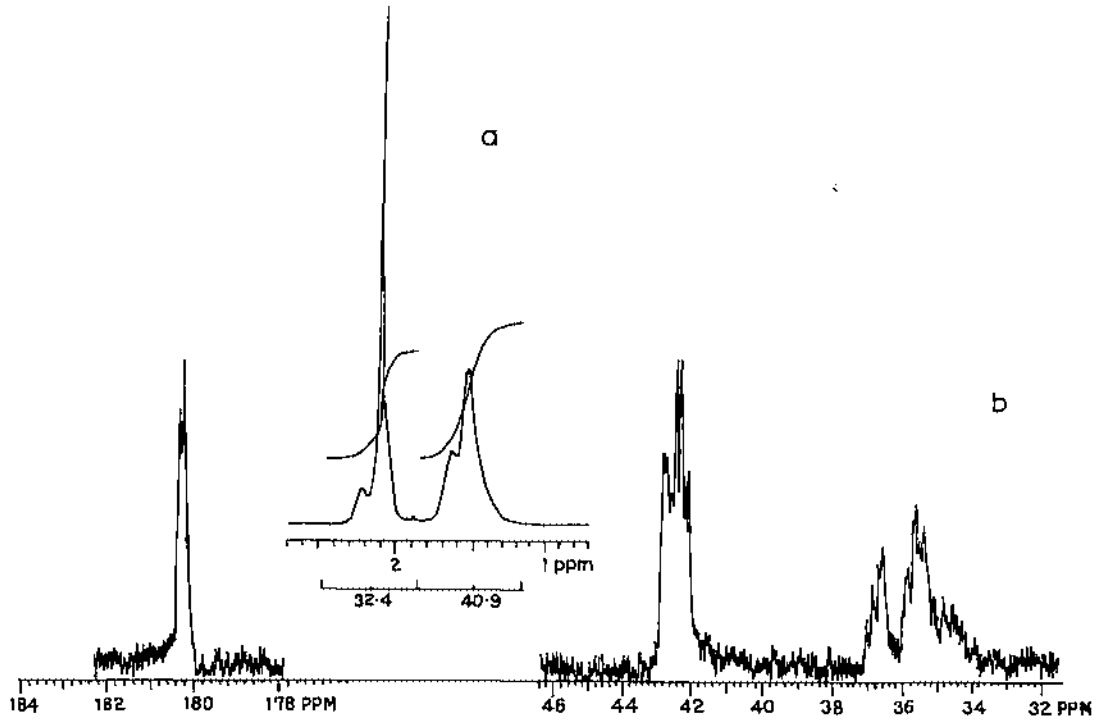

Figure 4 ^{1}H and ^{13}C n.m.r. spectra of thiourea terminated polyacrylamide formed on montmorillonite surfaces: (a) ^{1}H n.m.r. spectrum; (b) ^{13}C n.m.r. spectrum

XRD measurement

Unoriented powder samples of montmorillonite (H^+ and Fe(III) exchanged) before and after polymerisation reaction showed XRD patterns consistent with published results[10]. After the polymerisation reaction, the intensity of peak at $2\theta = 6.25°$ became much lower because of the presence of templates of polymer materials in the interlayer space. On the other hand, intensity of the peak at $2\theta = 9.5$–9.8 is increased due to polymerisation as well as glycerol treatment. Basal spacing of the H^+ and Fe(III) exchanged minerals is increased from 14 to 17 Å due to glycerol treatment for both TU treated and untreated samples. On the other hand, polymerisation increases basal spacing from 14 to 15 Å. Glycerol does not affect basal spacing at this stage. Foregoing results indicate that Fe(III) ions, TU and monomers all are intercalated between layers of the mineral without expanding the same and the locus of the polymerisation reaction is the interlayer spaces of the mineral. The location of Fe(III) ions in the interlayer space eventually retard the termination process, resulting in the higher degree of polymerisation.

^{1}H and ^{13}C n.m.r. spectra of PAM

^{1}H n.m.r. spectrum of PAM is not usually an well resolved spectrum and no special feature is apparent in present spectrum (*Figure 4a*) except that of overlapping of a sharp line with chemical shift of 2.12 ppm near the $-CHCONH_2$ position. This line in all probability represents the hydrogens from the isothiocarbamido end groups of thiourea terminated PAM. The expanded ^{13}C n.m.r. spectrum (*Figure 4b*) showed methylene, methine and carbonyl carbons of head-to-tail polymer of AM. No monomeric acrylamide was seen indicating purity of the polymer sample. The carbonyl carbon (at 180.2 ppm) splittings were small and not as readily interpreted as backbone carbon absorptions. The methine resonance

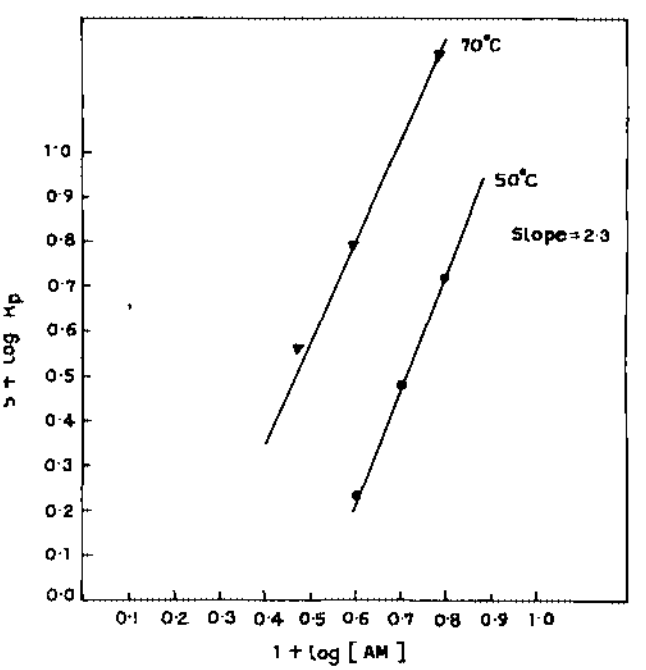

Figure 5 Logarithm plot of R_p *versus* [AM]: [Fe(III)] = 0.0015 mol l^{-1}, [TU] = 0.04 mol l^{-1}

(42.2–43.5 ppm) is a triplet (triad sensitivity) which is further split, showing pentade sensitivity. The low field and high field triplet peaks are assigned to rr (syndiotactic) and mm (isotactic) sequences, respectively. The central peak corresponds to heterotactic sequences (mr + rm). The methylene carbon lines (34–37.4 ppm) fall into three fairly well separated groups with almost all the 20 lines required by hexad sensitivity resolved. The resemblance of the

spectrum to those obtained by Lancaster and Coworker suggests that Bernoulli statistics are followed, which is common in vinyl polymers[20].

Kinetics and mechanism. In homogeneous reaction condition (i.e., in the absence of any clay mineral) R_p is decreased with increased Fe(III) ion concentrations (*Table 1*), which is consistent with previous reports on similar redox systems and supports linear termination hypothesis by the metal ions[12,14–17]. The rate dependence on the monomer (M) concentrations could be related to neither a first order nor a second order reaction and the slope of the logarithm plot of R_p *versus* [AM] was found to be 1.45 (not shown in figure). Referring to the literature concerned with other redox systems involving metals as oxidants, the above kinetic behaviour predicts a polymerisation mechanism similar to that reported earlier[16]. The variation of the initial rate of polymerisation as a function of monomer concentration in the presence of montmorillonite is shown in *Figure 5*. Not all the points fell on a linear line. If it is assumed to be linear, the slope could be estimated as about 2.3. (The proposed mechanism, however, predicts an exponent of 2.0, the error in the experimental data may be introduced from the inherent coarseness in following the kinetics of a heterogeneous system.) The significant change in the monomer exponent due to the occurrence of the reaction on the montmorillonite surface indicates that the polymerisation mechanism is greatly affected by the mineral microenvironment. A rate dependence of second order and above on monomer concentration was also observed earlier in heterogeneous and precipitation polymerisation of acrylamide and various interpretations, including 'cage effect' and 'complex theory', were proposed to account for the significant departure from first order kinetics[18,19]. The 'cage effect' suggests that when an initiator decomposes into two radicals, there is a formation of a potential barrier by the surrounding solvent molecules which prevent their immediate diffusion and favours their destruction by mutual recombination. The 'complex theory' is based on the formation of a complex between the initiator and the monomer, the rate of initiation then being determined by the rate of decomposition of the complex. The 'cage effect' seems to be a good conceptual starting point in explaining the high monomer exponent which has been observed in the present system. To examine the dependence of rate on the montmorillonite content and Fe(III) concentrations, the initial rate of polymerisation is plotted as a function of $\overline{Fe}$(III) ion concentration (*Figure 6*), R_p is increased with the montmorillonite and Fe(III) contents of the reaction mixture but the slope of logarithm plot varied from 0.25 to 0.40 as a result of raising the reaction temperature from 50 to 70°C. However, if the locus of polymerisation is assumed to be the interlayer space of montmorillonite, above slopes can not be regarded as metal ion exponents because increasing addition of Fe(III)-saturated mineral does not increase Fe(III) ion concentration in the mineral phase but, on the contrary, only

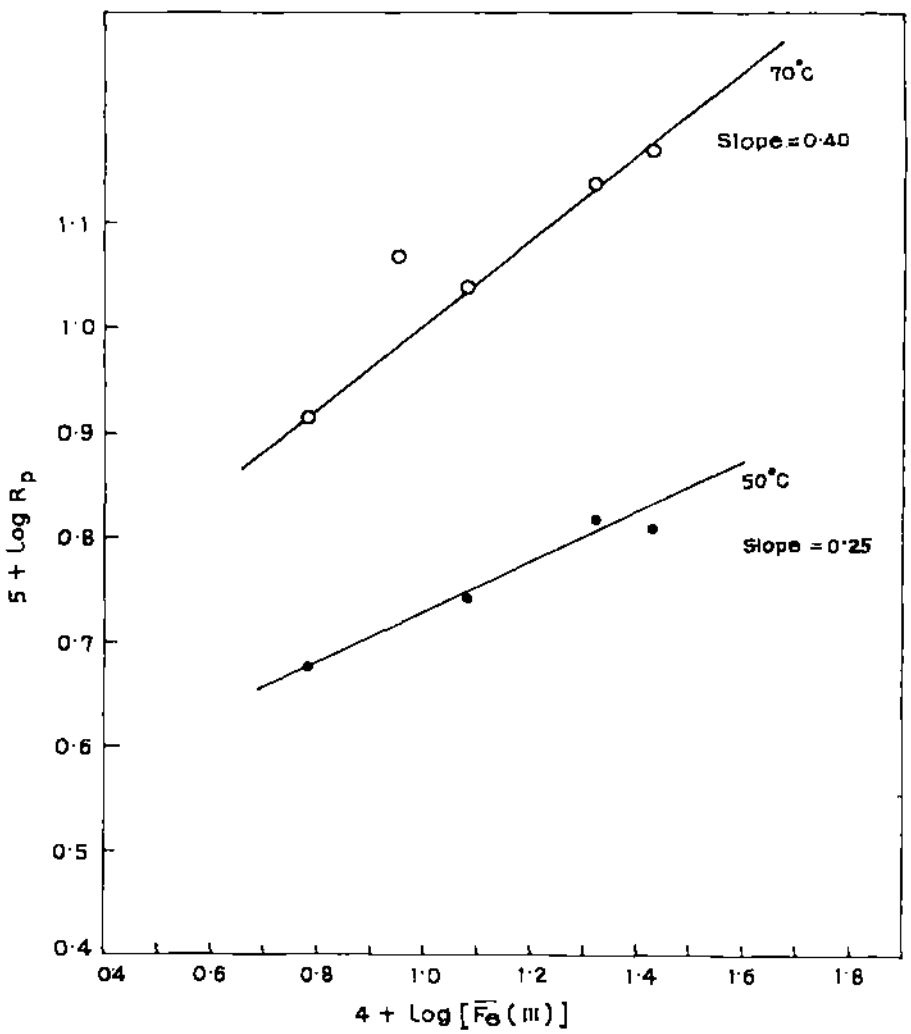

Figure 6 Logarithm plot of R_p *versus* [Fe(III)]: [AM] = 0.4 mol l^{-1}, [TU] = 0.04 mol l^{-1}, [Mo] = 0.5%

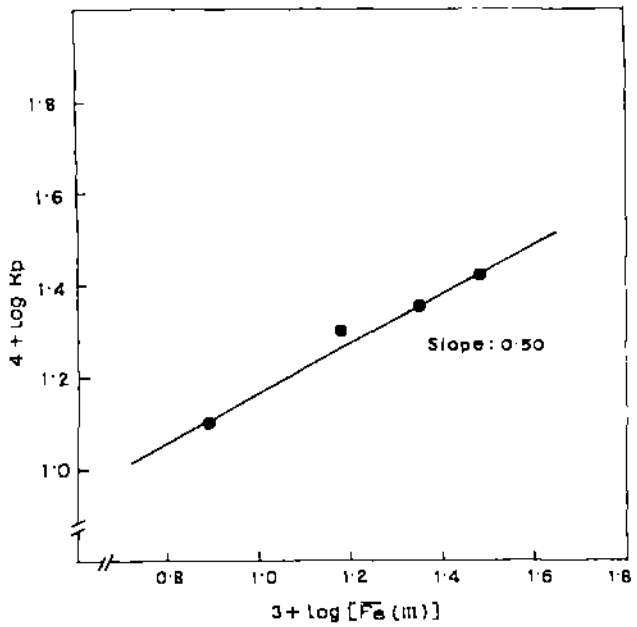

Figure 7 Logarithm plot of R_p *versus* [$\overline{Fe}$(III)]: [AM] = 0.4 mol l^{-1}, [TU] = 0.04 mol l^{-1}, [Mo] = 0.5% ([Fe(III)] in this figure represents moles of ferric ions in the montmorillonite gel phase)

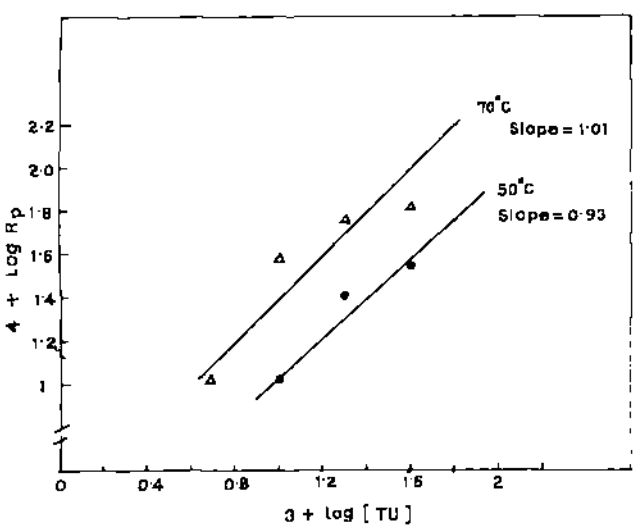

Figure 8 Logarithm plot of R_p *versus* [TU]: [Fe(III)] = 0.0015 mol l^{-1}, [AM] = 0.4 mol l^{-1}, [Mo] = 0.5%

adds to the total metal ion and adsorbent contents of the reaction mixture. This in turn increases monomer and TU contents of the intercalate position, which result in the high rates of polymer yield. In order to measure the actual metal exponent for the reaction in the mineral phase, R_p values were plotted as a function of Fe(III) ion concentration in the montmorillonite gel. The concentrations of Fe(III) in the montmorillonite gel were varied by adding calculated quantities of HM in the reaction mixture. The slope of such a logarithm plot (*Figure 7*) has been estimated as 0.50 at 50°C. (The concentration of Fe(III) now being moles of interlayer Fe(III) ions per 1000 mL montmorillonite gel; the water content of montmorillonite sample was measured following the method described by Marinsky and co-workers and found to be 10 ml g^{-1})[21]. *Figure 8* shows the dependence of R_p on TU concentrations. Since the isothiocarbamido primary radicals (I) have strong tendency to dimerise above 0.05 mol l^{-1}, the present study was confined below that concentration only[8]. Again, not all the points fell on a linear line (in the logarithm plot) owing to the heterogeneous reaction mixture. However, the slopes of the average lines drawn through the points at two different temperatures indicate that the reaction is first order with respect to TU concentrations. To rationalise the above experimental results and to predict a possible mechanism for the seemingly complex polymerisation reaction occurring in the mineral microenvironment, the following assumptions are made[12,22].

(1) Intercalated TU reacts fast with the Fe(III) ions of montmorillonite layered spaces to form the reactive TU (isothiocarbamido (I)) radicals via an intermediate complex. The decomposition of the complex is the rate-controlling step.

(2) In the acidic and metal ion exchanged aqueous montmorillonite system, a fraction of the intercalated acrylamide molecules are present near reacting sites as pairs either through hemisalts formation, where two amide molecules share a proton by means of symmetrical hydrogen bond or/and through weak coordination to the exchanged cations[2]. The protonated as well as the complexed amide pairs are at fast equilibrium with unprotonated and free amide molecules, respectively, which are defined by a protonation constant or a formation constant. In view of high monomer exponent, it is certain that it must have resulted in part from the involvement of monomer in the initiation step, where such monomer pairs are entailed.

(3) Since the reactive TU radicals are formed as pairs, assumption of the 'cage effect' seems to be conceptually appropriate. The initiation step involves collision of the 'amide pairs' with caged TU radicals at the wall of the cage and random diffusion of the radicals from the cage and their secondary recombination are less significant in comparison with the rate of dimerisation of caged radicals or their reaction with acrylamide.

Initiation

$$\overline{Fe}(III) + TU \overset{K}{\rightleftharpoons} \underset{Complex}{\overline{Fe}(III) - TU} \tag{1}$$

$$\overline{Fe}(III) - TU + TU \xrightarrow{k_i} \overline{Fe}(II) + (2TU^{\cdot}) + H^+ \tag{2}$$

$$(TU^{\cdot}) + M_2H^+ \xrightarrow{k_i} M_1^{\cdot} + M + H^+ \tag{3}$$

Propagation

$$M_1^{\cdot} + M \xrightarrow{k_p} M_2^{\cdot}$$

$$M_{n-1}^{\cdot} + M \xrightarrow{k_p} M_n^{\cdot} \ldots \text{etc.} \tag{4}$$

Termination

$$M_n^{\cdot} + M_n^{\cdot} \xrightarrow{k_t} M_n - M_n \tag{5}$$

$$(TU^{\cdot}) + \overline{Fe}(III) \xrightarrow{k_t'} TU + \overline{Fe}(II) \tag{6}$$

$$(2TU^{\cdot}) \xrightarrow{k_t''} TU - TU \tag{7}$$

(caged species are enclosed in brackets)

Using the above scheme and the pseudo-steady-state assumption, we derive the rate expressions as follows:

$$\frac{-\mathrm{d}[\overline{\mathrm{Fe}}(\mathrm{III})]}{\mathrm{d}t} = \frac{k_\mathrm{d}K[\mathrm{TU}]^2[\overline{\mathrm{Fe}}(\mathrm{III})]}{1+K[\mathrm{TU}]} \tag{8}$$

$$R_\mathrm{p} = \frac{(k_\mathrm{d}k_\mathrm{i}KK')^{1/2}k_\mathrm{p}[\overline{\mathrm{Fe}}(\mathrm{III})]^{1/2}[\mathrm{TU}][\mathrm{M}]^2}{k_\mathrm{t}^{1/2}(k_\mathrm{i}K'[\mathrm{M}]^2 + k_\mathrm{i}KK'[\mathrm{M}]^2[\mathrm{TU}] + k_\mathrm{t}'[\overline{\mathrm{Fe}}(\mathrm{III})] + k_\mathrm{t}''(1+K[\mathrm{TU}]))^{1/2}} \tag{9}$$

(K' ($= [\mathrm{M_2H^+}]/[\mathrm{M}]^2$) is the apparent protonation constant at a fixed pH (or a formation constant))

If the oxidative termination (step 6) is assumed to be insignificant in comparison with the dimerisation rate of caged radicals, equation (9) reduces to:

$$R_\mathrm{p} = \frac{(k_\mathrm{d}k_\mathrm{i}KK')^{1/2}k_\mathrm{p}[\overline{\mathrm{Fe}}(\mathrm{III})]^{1/2}[\mathrm{TU}][\mathrm{M}]^2}{k_\mathrm{t}^{1/2}(k_\mathrm{i}K'[\mathrm{M}]^2 + k_\mathrm{i}KK'[\mathrm{M}]^2[\mathrm{TU}] + k_\mathrm{t}''(1+K[\mathrm{TU}]))^{1/2}} \tag{10}$$

The interpretation of high kinetic order of the monomer finally hinges on the dominance of a reaction between caged radicals and those of monomers with the radicals at the cage wall. Although the concentrations of the monomer and TU in solution phase were fixed mostly at 0.40 mol l^{-1} and 0.04 mol l^{-1} respectively, the concentrations of intercalated species must be much lower, specially due to the presence of water molecules in the interlayer spaces.

Thus, while the concentrations, [M] and [TU], in the montmorillonite gel-phase should be

$$[\mathrm{M}] = L_\mathrm{o}^\mathrm{a}\theta_\mathrm{m} = \frac{L_\mathrm{o}^\mathrm{a}K_\mathrm{m}^\mathrm{a}[\mathrm{M}]_\mathrm{s}}{1+K_\mathrm{tu}^\mathrm{a}[\mathrm{TU}]_\mathrm{s}+K_\mathrm{m}^\mathrm{a}[\mathrm{M}]_\mathrm{s}} \tag{11}$$

and,

$$[\mathrm{TU}] = L_\mathrm{o}^\mathrm{a}\theta_\mathrm{tu} = \frac{L_\mathrm{o}^\mathrm{a}K_\mathrm{tu}^\mathrm{a}[\mathrm{TU}]_\mathrm{s}}{1+K_\mathrm{tu}^\mathrm{a}[\mathrm{TU}]_\mathrm{s}+K_\mathrm{m}^\mathrm{a}[\mathrm{M}]_\mathrm{s}} \tag{12}$$

(subscript 's' denotes solution)

(L_o^a and θ are the total active sites in unit mass of montmorillonite and the fraction of total sites occupied by each species respectively; K_m^a and K_tu^a are selectivity coefficients)

the denominators of equations (11) and (12) are nearly unity. By appropriate substitution of [M] and [TU] in equation (10) and considering the dominance of the last term of the denominator over others, the equation becomes

$$R_\mathrm{p} = \frac{k_\mathrm{p}(k_\mathrm{d}k_\mathrm{i}KK'/k_\mathrm{t}k_\mathrm{t}'')^{1/2}K_\mathrm{tu}^\mathrm{a}(K_\mathrm{m}^\mathrm{a})^2(L_\mathrm{o}^\mathrm{a})^3[\overline{\mathrm{Fe}}(\mathrm{III})]^{1/2}[\mathrm{TU}]_\mathrm{s}[\mathrm{M}]_\mathrm{s}^2}{(1+KL_\mathrm{o}^\mathrm{a}K_\mathrm{tu}^\mathrm{a}[\mathrm{TU}]_\mathrm{s})^{1/2}} \tag{13}$$

(Values of K_m^a (or K_tu^a), L_o^a and K are of the order of 10^{-2}, 2 mmol g^{-1} and 2 l mol^{-1}, respectively[22,23]. Small values of above parameters including that of K', ensure that terms involving quadratic and above concentrations are very small in the present conditions[24,25]).

Further inspection of equation (13) shows that the value of $KL_\mathrm{o}^\mathrm{a}K_\mathrm{tu}^\mathrm{a}$ $[\mathrm{TU}]_\mathrm{s}$ in the denominator varies from 10^{-5} to 10^{-6} for the variation of aqueous TU concentration from 0.05 to 0.005 mol l^{-1}. This implies that the rate equation under the present condition is reduced to

$$R_\mathrm{p} = k_\mathrm{p}(k_\mathrm{d}k_\mathrm{i}KK'/k_\mathrm{t}k_\mathrm{t}'')^{1/2}K_\mathrm{tu}^\mathrm{a}(K_\mathrm{m}^\mathrm{a})^2(L_\mathrm{o}^\mathrm{a})^3[\overline{\mathrm{Fe}}(\mathrm{III})]^{1/2}[\mathrm{TU}]_\mathrm{s}[\mathrm{M}]_\mathrm{s}^2 \tag{14}$$

Reviewing the above result, we find that equation (14) could satisfactorily account for the present behaviour of the $\overline{\mathrm{Fe}}$(III)–TU initialised acrylamide polymerisation exhibited in the aqueous montmorillonite layered space.

CONCLUSIONS

Aqueous polymerisation of acrylamide by Fe(III)–thiourea redox couple shows kinetic behaviour and mechanism similar to those of other redox initiated polymerisations of acrylamide. On the other hand, polymerisation initiated by the same redox couple but by loading Fe(III) ions in the interlayer spaces of montmorillonite influences the kinetics as well as the mechanism to a great extent. The latter technique increases the degree of polymerisation and the intrinsic viscosity of the polymers dramatically by decreasing the rate of linear termination process. The method was demonstrated to be a promising technique of achieving high molecular weight polymers for redox initiated reactions, where low molecular weight polymers are often displayed. The maximum values of $\bar{M}_\mathrm{v}$ were found to be 2.6×10^5 and 2.5×10^6 in the absence and presence of montmorillonite respectively, while η values increased from 108 to 595 ml g^{-1} due to the presence of the mineral under identical condition. E.s.r. study confirms that lattice substituted Fe(III) in montmorillonite reacts with thiourea but the reaction failed to initiate polymerisation of acrylamide in water. The locus of the polymerisation was identified by XRD as the interlayer space of the mineral while, the propagating radicals were characterised by spin-trapping technique. The hyperfine splitting parameters a_N and a_H^β for the MNP adduct are 1.45 and 0.31 mT respectively. The polymers, characterised by ^{1}H and ^{13}C n.m.r., were mostly thiourea terminated head-to-tail polymers with mixed tacticities where Bernoulli statistics were followed. The kinetics study showed the monomer, TU and the metal ion exponents to be 2.0, 1.0, and 0.5 respectively, which have been explained by means of a radical mechanism involving 'cage effect' on the initiating TU radical pairs. In view of the presence of acrylamide molecules as hemisalts where two amide molecules share a proton through a symmetrical hydrogen bond in the acidic montmorillonite layered space, the initiation step probably involves collision of caged TU radicals with the monomer pairs at the cage wall.

ACKNOWLEDGEMENTS

Authors are thankful to CSIR, New Delhi for financial support.

REFERENCES

1. Theng, B. K. G., *Clay and Clay Minerals*, 1982, **30**, 1.

2. Theng, B. K. G., *The Chemistry of Clay-organic Reactions*, 1974, Adam-Hilger, London.
3. Bhattacharya, J., Chakravarti, S. K., Talapatra, S., Saha, S. K. and Guhaniyogi, S. C., *Journal of Polymer Science, Part A: Polymer Chemistry*, 1989, **27**, 3977.
4. Talapatra, S., Saha, S. K., Chakravarti, S. K. and Guhaniyogi, S. C., *Polymer Bulletin*, 1983, **10**, 21.
5. Jackson, M. L., *Soil Chemical Analysis*, 1973, Prentice Hall of India(P) Ltd., New Delhi.
6. François, J., Sarazin, D., Schwartz, T. and Weill, G., *Polymer*, 1979, **20**, 969.
7. Candau, F., Leong, Y. S., Pouyet, G. and Candau, S., *Journal of Colloid and Interface Science*, 1984, **101**, 167.
8. Saha, S. K. and Greenslade, D. J., *Bulletin of the Chemical Society of Japan*, 1992, **65**, 2720.
9. Solomon, D. H., Loft, B. C. and Swift, J. C., *Clay Minerals*, 1968, **7**, 389.
10. Fripiat, J. J., *Development in Sedimentology*, 1982, Elsevier, New York.
11. Bhattacharya, J., Saha, S. K. and Guhaniyogi, S. C., *Journal of Polymer Science, Part A: Polymer Chemistry*, 1990, **28**, 2249.
12. Hsu, W. C., Kuo, J. F. and Chen, C. Y., *Journal of Polymer Science, Part A: Polymer Chemistry*, 1993, **31**, 267.
13. McGrath, J. E., *Journal of Chemical Education*, 1981, **58**, 844.
14. Misra, G. S. and Bhattacharya, S. N., *Journal of Polymer Science, Polymer Chemistry Edition*, 1982, **20**, 131.
15. Balakrishnan, T. and Subbu, S., *Journal of Polymer Science, Part A: Polymer Chemistry*, 1986, **24**, 2271.
16. Hsu, W. C., Kuo, J. F. and Chen, C. Y., *Journal of Polymer Science, Part A: Polymer Chemistry*, 1992, **30**, 2459.
17. Hsu, W. C., Chen, C. Y., Kuo, J. F. and Wu, E. M., *Polymer*, 1994, **35**, 849.
18. Tai, E. F., Caskey, J. A. and Allison, B. D., *Journal of Polymer Science, Part A: Polymer Chemistry*, 1986, **24**, 567.
19. Riggs, J. P. and Rodriguez, F., *Journal of Polymer Science, Part A1*, 1967, **5**, 3151.
20. Lancaster, J. E. and O'Connor, M. N., *Journal of Polymer Science, Polymer Letters*, 1982, **20**, 547.
21. Marinsky, J. A., Lin, F. G. and Chung, K. S., *Journal of Physical Chemistry*, 1983, **87**, 3139.
22. Pustelnik, N. and Soloniewiez, R., *Chemia Analityczna (Warsaw)*, 1976, **21**, 503.
23. Bera, P. and Saha, S. K., unpublished results.
24. Perrin, D. D., *Organic Ligands: IUPAC Chemical Data Series (No. 22)*, 1983, Pergamon Press, New York.
25. Martell, A. E. and Smith, R. M., *Critical Stability Constant*, Vol. 3, 1979, Plenum Press, New York.

Indian Journal of Chemical Technology
Vol. 6, January 1999, pp. 24-30

Selective trapping of initiator component in the interlayer space of montmorillonite : A novel technique of controlling linear termination in aqueous acrylamide polymerisation

P Bera & S K Saha

Department of Chemistry, University of North Bengal, Darjeeling 734 430, India

Received 18 August 1998; accepted 11 December 1998

Kinetics and mechanism of aqueous polymerization of acrylamide by $FeCl_3$ -thiourea redox couple are investigated in homogeneous solution with a view to compare results with those observed after trapping metal oxidant in the montmorillonite layered space. The initial rate of polymerization and the intrinsic viscosity are ranged within $(0.3\text{-}2.3) \times 10^4$ mol L^{-1} s^{-1} and (14-137) mLg^{-1} respectively in the former case. Linear termination by metal oxidants is checked in the latter instance resulting in the higher chain growth of the polymers. Formation of the acrylamide pairs in the interlayer positions of acidic montmorillonite, strong 'cage effect' on the initiating thiourea radicals and the delayed termination process are identified as the major causes for the observed mechanistic modification in the montmorillonite gel phase reactions.

Polyacrylamide with high molecular weights and intrinsic viscosities have found applications as water soluble viscofier and displacement fluid in secondary oil recovery[1]. High molecular weight polyacrylamides have such other applications as effective flocculants and chemical grouts. Redox initiated polymerization of acrylamide is one of the most common techniques applied for aqueous polymeri-zation because of the simplicity of technique as well as high yield and reaction rates. Moreover, the above technique is uniquely applied for *in situ* polymerization, where aqueous solutions of the monomer together with a redox catalyst are injected into soil formation. However, one major difficulty of such a technique is the fast termination by oxidant of the redox couple. In an attempt to increase the chain length of polyacrylamide initiated by a redox couple, the potential electron acceptor of the redox couple (e.g., metal ions) is loaded into the interlayer space of montmorillonite[2,3]. This ensures the slow termination due to the inability of a growing polymer chain to transfer to the oxidant trapped inside the layered space. As a result, high molecular weight polymers were formed. However, the effect of montmorillonite micro-environment in the above polymerization was not confined to the lowering of termination rates only but, it affected the mechanism of the reaction also to a great extent. In order to examine various aspects pertaining to such modifications, the kinetics and mechanism of solution polymerization of acrylamide by $FeCl_3$/thiourea system have also been studied. In the present paper, the results of these experiments have been reported and an attempt has been made to identify the pathways through which above modifications are achieved.

Experimental Procedure

Materials

Acrylamide (AM, reagent grade, Fluka) was purified by recrystallization from methanol (two times) and dried in vacuum oven at 45 °C overnight. Thiourea (TU, E.Merck) was used after recrystallization three times from distilled water (m.p. 180°C). A suspension of montmorillonite (MO) having particle size less than 2 micron (diameter) was prepared by sedimentation. Free iron oxides were removed by dithionite-citrate method. Organic matters were removed following method described elsewhere[4]. H^+-montmorillonite (HM) was prepared by shaking the stock of the mineral (3% w/v) in the presence of 0.5 M HCl for about 6 h followed by repeated centrifugation (20,000 rpm) and washing with double distilled water. The cation exchange capacity (CEC) of montmorillonite was determined by potentiometric titration with standard KOH solution under nitrogen atmosphere and was found to be 0.91 meq./g. Fe(III)- montmorillonite (FeM) was prepared by shaking HM suspension (3% w/v) in the presence of 0.5 M $FeCl_3$ (reagent grade) at *p*H 2.5 for 6 h followed by purification by repeated centrifu-

gation and washing with distilled water until the test of Fe(III) ions in the supernatent was negative. A separate experiment on the sorption of Fe(III) on to montmorillonite showed that the maximum intake of Fe(III) ions by HM sample slightly exceeded the CEC value, viz., 0.98 meq/g.

Sorption of TU and AM on montmorillonite

10 mL portions of a 0.5% suspension of HM were placed in a number of pyrex bottles and different amounts of either thiourea or acrylamide were added followed by adjusting the *p*H to 2.0 with dil HCl. The total volume of the suspension was made up to 15 mL in each case by adding the requisite amount of water and were shaken at 30 °C for 4 h to attain equilibrium. The supernatent solutions were then centrifuged (20,000 rpm) and analysed for TU or AM by a Shimadzu UV-vis spectrophotometer at 235 and 195 nm respectively.

Potentiometric measurement

The redox behaviour of Fe(III)-TU and FeM-TU systems were examined by potentiometric titration of either $FeCl_3$ solution or FeM suspension with TU. The electrochemical cells were simple as shown below:

Pt/Fe(III) (or Fe(III)M), Fe(II) (or Fe(II)M)// KCl, $HgCl_2$,Hg/Pt

A stoppered pyrex beaker fitted with nitrogen gas inlet-outlet tubes, Pt-electrode, salt bridge and mechanical stirring arrangements was placed in a thermostat at 50°C. 20 mL $FeCl_3$ solution or FeM suspension was then titrated at *p*H 2.0 with standard thiourea solution under nitrogen atmosphere.

Polymerization

Measured quantities of aqueous solution of AM were added to known amounts of $FeCl_3$ solution or FeM and HM mixtures in well stoppered pyrex bottles under nitrogen atmosphere and were equilibrated at required temperature. Deaerated TU solutions were then added to these solutions and the reactions were allowed to continue for desired time span in absence of any light. Polymerization reactions were stopped by diluting the mixture with chilled water keeping the reaction vessel in ice bath. The mixtures were then centrifuged to remove HM or FeM, if any. The polyacrylamide was precipitated out by adding excess of acetone, washed repeatedly with acetone and dried in vacuum at 40°C for 48 h. Molecular weights of the polymers were determined by viscosity measurement in aqueous 0.1M NaCl solution using a Ubbelohde viscometer and a Mark-Houwink relationship of the type[5,6]:

$[\eta]=9.33\times10^{-3} M^{0.75}$ cc/g.

Results and Discussion

Table 1 shows data pertaining to the aqueous homogeneous polymerization of acrylamide by $FeCl_3$/TU redox initiator. The molecular weight (M_v) of the polymer obtained was ranged between 0.2×10^5–3.6×10^5. The initial rate of polymerization, R_p, was moderately high and ranged between 3×10^{-5}–17×10^{-5} mol $L^{-1}s^{-1}$. At a fixed TU and AM concentrations, all the parameters, viz., R_p, X_L, $[\eta]$ and M_v were decreased with the increase in Fe(III) concentrations of the initiating redox couple. It seems apparent that the Fe(III) ions are not only involved in

Table 1 — The initial rates of polymerization, polymer yields, intrinsic viscosities and the molecular weights of $FeCl_3$/TU initiated polymerization of acrylamide at various conditions

$[FeCl_3]$ mM	[TU] M	[AM] M	*p*H	Temp °C	$R_p\times10^5$ mol $L^{-1}s^{-1}$	X_L [a] %	$[\eta]$ $mL.g^{-1}$	$M_v\times10^5$
1.5					17.2	73	64	1.3
3.0	0.04	0.4	2.01	50	9.4	56	73	1.5
4.0					6.7	40	61	1.2
8.0					4.2	26	45	0.8
	0.01				2.9	40	14	0.2
1.5	0.02	0.4	2.01	50	5.7	53	68	1.4
	0.03				11.9	68	73	1.6
		0.3			8.3	62	60	1.2
1.5	0.04	0.5	2.01	50	20.0	81	96	2.2
		0.6			23.0	77	108	2.6
				45	12.6	68	61	1.2
1.5	0.04	0.4	2.01	60	27.8	75	74	1.6
				70	19.2	86	137	3.6

[a]polymer yield after 4.5 h.

the termination process but also act as retarder in the reaction[7]. Linear termination of aqueous acrylamide polymerization by Fe(III) ions was observed long back in 1957 when aqueous Fe(III) perchlorate caused fast termination of x - and γ-ray initiated polymerization of acrylamide with a rate constant of $1.1\pm0.6\times10^4$ L $mol^{-1}s^{-1}$ (Ref.7). Similar role of other metal oxidants was also observed subsequently.

Effect of AM, TU and Fe(III) concentrations

The rate of polymerization, R_p, as well as the polymer yield (X_L) decrease with the increasing Fe(III) ion concentration in the range of 1.5×10^{-3}–8.0×10^{-3} mol L^{-1}. The value of the metal ion exponent, obtained from the slope of the double logarithmic plot of R_p versus metal concentration is found to be 0.90 (Fig. 3). Thus, the rate is inversely proportional to nearly first power of metal ion concentration. On the other hand, R_p increases with increasing concentration of thiourea. Thiourea alone (in absence of Fe(III) ions) is incapable of initiating polymerization as the control experiment shows. Increasing concentration of the activator (thiourea) in

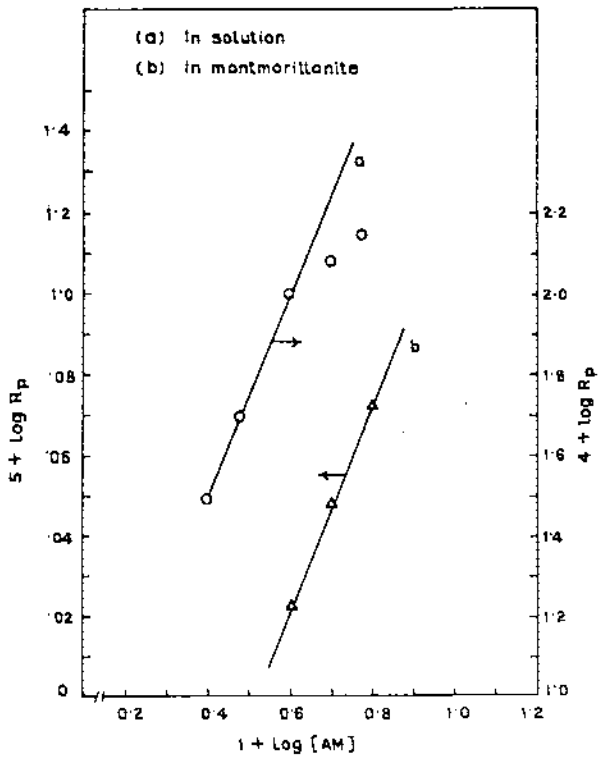

Fig. 1 — Logarithm plots of R_p *versus* [AM] for the polymerization reaction in solution as well as MO phase; $[FeCl_3]=1.5\times10^{-3}$M, [TU]=0.04M and [Fe(III)] $=1.5\times10^{-3}$M.

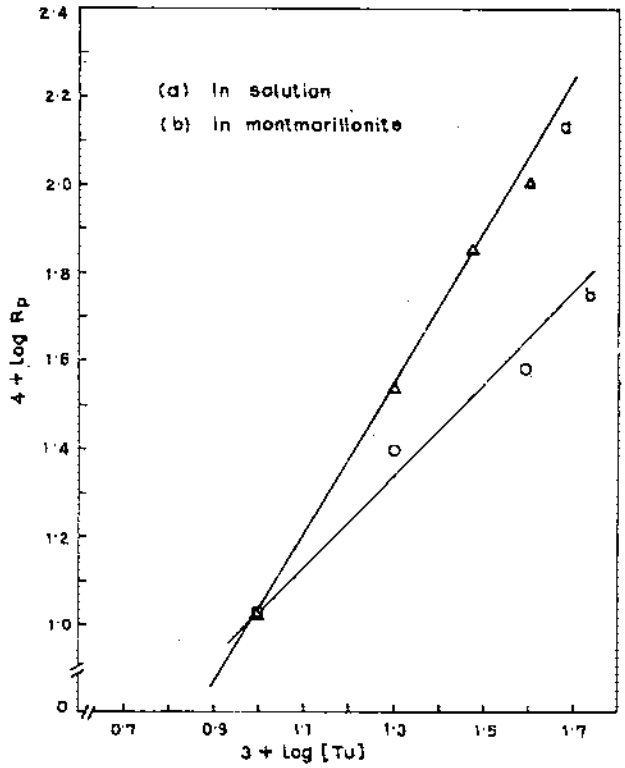

Fig. 2 — Logarithm plots of R_p *versus* [TU] for the polymerization reaction in solution as well as MO phase; $[FeCl_3]=1.5\times10^{-3}$M, [AM]=0.4M and [Fe(III)]$=1.5\times10^{-3}$M.

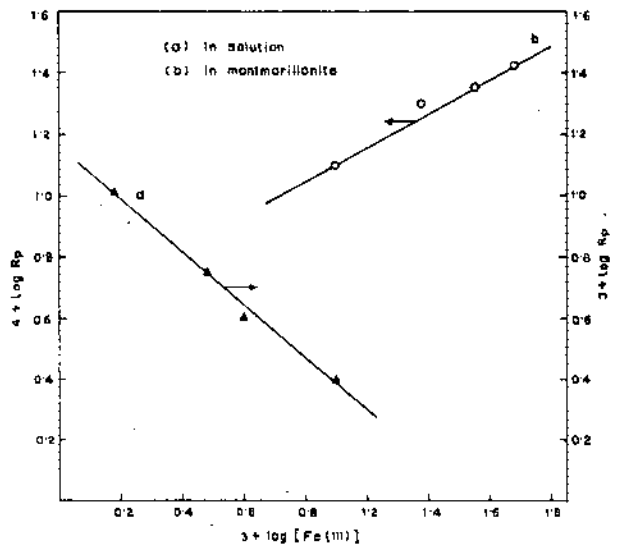

Fig. 3 — Logarithm plots of R_p *versus* [Fe(III)] for the polymerization reaction in solution as well as MO phase; [AM]=0.4M and [TU]=0.04M (for the MO-phase reaction, [Fe(III)] in the figure represents moles of ferric ions in 1000 mL of MO gel).

the presence of Fe(III) ions increases the concentration of the initiating radical and consequently the number of propagating polymer chains and hence the rate of polymerization increases with increasing TU concentration in the range 0.01-0.04 mol L^{-1}. However, at still higher concentrations of TU, R_p as well as X_L tend to decrease considerably due to increase in the rate of termination via dimerization of isothiocarbamido primary radicals (TU)[8]. The value of TU exponent obtained from the slope of the double logarithmic plot of R_p versus TU concentration, is 1.8 (Fig. 2). Thus, the rate of polymerization shows nearly second order dependence on the TU concentration. The dependence of R_p on the monomer concentration is, however, interesting. The initial rate increases with the increase of monomer concentration as expected. The slope of the logarithmic plot of R_p versus concentration of AM is nearly 2.0 (Fig.1) in the range of AM concentration of 0.25-0.40 mol L^{-1}, but tends to decrease (the value becomes 1.0, experimental points shown in Fig.1) in the higher concentration range of (0.4-0.6) mol L^{-1} (explained under kinetics and mechanism). The corresponding plots for the MO gel phase reactions are shown in the Figs 1-3. The data are taken from ref. 3 and reproduced here for comparison.

Effect of temperature

The R_p as well as X_L increase with increasing polymerization temperature. However, the R_p value tend to decrease at temperature above 60°C. The overall energy of activation as calculated from the Arrhenius plot has been found to be 12.4 kcal.mol^{-1} within the temperature range 45-60 °C.

Kinetics and mechanism

In order to rationalize the results, following assumptions are made to predict the mechanism of aqueous homogeneous polymerization of acrylamide by $FeCl_3$/TU system.

1. Isothiocarbamido (TU) primary radicals are formed via an intermediate complex between Fe(III) ions and TU. The decomposition of the complex is the rate-determining step[9,10]

$$\mathrm{Fe(III) + TU} \underset{\text{Complex}}{\overset{K}{\rightleftharpoons}} \mathrm{Fe(III)\text{-}TU} \qquad \ldots(1)$$

$$\mathrm{Fe(III) - TU + TU} \xrightarrow{k_d} \mathrm{Fe(II) + (2TU^{\cdot}) + H^{+}} \qquad \ldots(2)$$

2. Since the reactive TU radicals are formed as pairs, assumption of "cage effect" seems to be conceptually appropriate. The initiation step involves collision of acrylamide molecule with caged TU radicals at the wall of the cage and random diffusion of the radicals from the cage and their secondary recombination are less significant.

Initiation :

$$(\mathrm{TU}^{\cdot}) + \mathrm{M} \xrightarrow{k_i} \mathrm{M}_1^{\cdot} \qquad \ldots(3)$$

Propagation :

$$\mathrm{M}_1^{\cdot} + \mathrm{M} \xrightarrow{k_p} \mathrm{M}_2^{\cdot}$$

$$\mathrm{M}_{n-1}^{\cdot} + \mathrm{M} \xrightarrow{k_p} \mathrm{M}_n^{\cdot} \ldots\ldots \text{etc.} \qquad \ldots(4)$$

Termination :

$$\mathrm{M}_n^{\cdot} + \mathrm{Fe(III)} \xrightarrow{k_t} \mathrm{M}_n + \mathrm{Fe(II)} \qquad \ldots(5)$$

$$(\mathrm{TU}^{\cdot}) + \mathrm{Fe(III)} \xrightarrow{k_t'} \mathrm{TU} + \mathrm{Fe(II)} \qquad \ldots(6)$$

$$(2\mathrm{TU}^{\cdot}) \xrightarrow{k_t''} \mathrm{TU\text{-}TU} \qquad \ldots(7)$$

(Caged species are enclosed in brackets)

Using Eqs (1) and (2), one obtains the consumption rate of Fe(III) concentration as

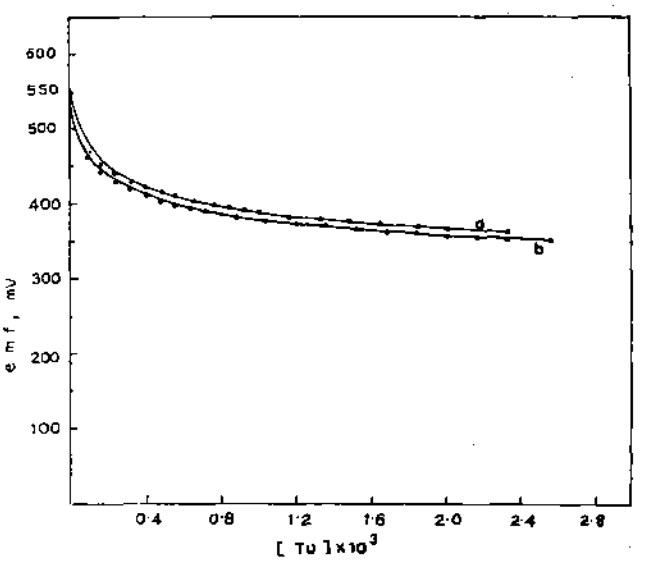

Fig. 4 — Potentiometric titrations of (a) FeM (1.3×10^{-3}M in terms of exchanged Fe(III) per 1000ml of suspension) versus TU; (b) $FeCl_3$ (1.2×10^{-3}M) versus TU.

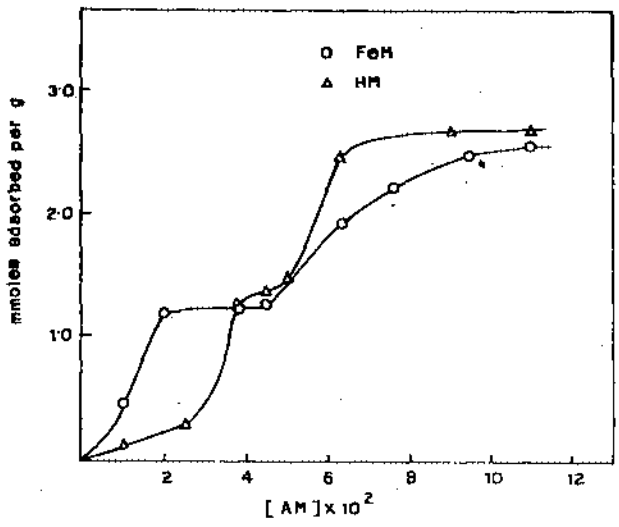

Fig. 5 — Adsorption isotherms of acrylamide on Fe - and H-montmorillonite.

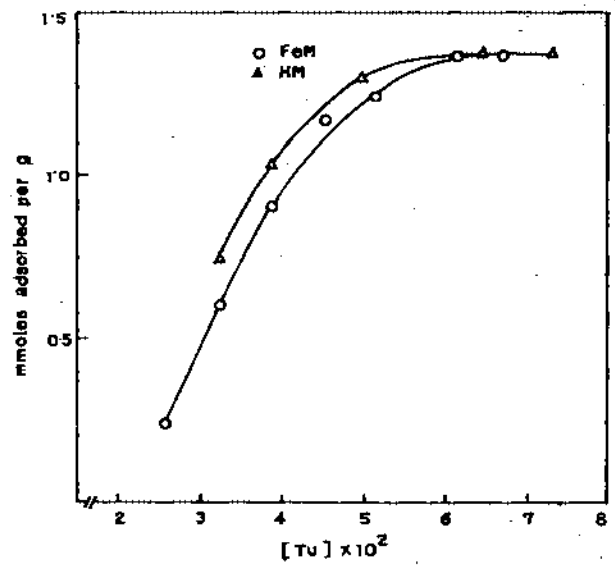

Fig. 6 — Adsorption isotherms of thiourea on Fe- and H-montmorillonite.

Table-2 — The initial rates of polymerization, polymer yields, intrinsic viscosities and the molecular weights of Fe(III)/TU initiated polymerization in montmorillonite phase

Fe(III)[a] mM	[TU] M	[AM] M	*p*H	Temp °C	$R_p \times 10^5$ mol $L^{-1}s^{-1}$	X_L[b] %	$[\eta]$ mL.g^{-1}	$M_v \times 10^5$
1.50	0.04	0.4	2.01	50	4.40	76	369	13.5
2.67	0.04	0.4	2.01	50	6.50	60	291	9.8
1.50	0.01	0.4	2.01	50	1.70	42	487	19.5
1.50	0.04	0.6	2.01	50	9.20	57	480	19.1
1.50	0.04	0.4	2.01	70	6.60	94	220	6.8
1.50	0.04	0.4	2.87[c]	70	—	—	—	—

[a] Concentration of interlayer Fe(III) in mmol. per litre of the reaction mixture (corresponding concentration in MO gel phase is 0.03 mol. per litre of MO gel);
[b] Yield after 4.5h; [c] no polymer formed.

$$-\frac{d[Fe(III)]}{dt} = \frac{k_d K [TU]^2 [Fe(III)]}{1 + K[TU]} \quad \ldots (8)$$

Assuming that the rate of consumption of Fe(III) ions is equal to the rate of formation of TU radicals and a pseudo-steady state approximation to hold, R_p may be shown as follows :

$$R_p = \frac{k_d k_i k_p K [TU]^2 [M]^2}{k_t (k_i[M] + k_t'[Fe(III)] + k'')(1 + K[TU])} \quad \ldots (9)$$

Since the concentration of TU throughout the experiment is low and the value of the equilibrium constant, K is only of the order of 2 L mol^{-1}, the quantity $(1+K[TU])$ in the denominator may approximately be equated to unity. Hence, the Eq (9) is reduced to

$$R_p = \frac{k_d k_i k_p K [TU]^2 [M]^2}{k_t (k_i[M] + K_t'[Fe(III)] + k'')} \quad \ldots (10)$$

Plotting of $[TU]^2[M]^2/R_p$ versus [M] yield a straight line. From the slope and the intercept of the plot the values of $k_t/k_p k_d$ and k_t'/k_i are found as 4.70 and 2.80×10^2 respectively. Reviewing the experimental results it seems apparent that k_t'' in the present homogeneous polymerization is not significant enough in comparison to other terms in the denominator of Eq.(10). Moreover, high value of k_t'/k_i ratio ensures that $k_i[M]$ is also insignificant at low [M] in comparison to the second term in the bracket of the denominator. Thus, Eq. (10) could satisfactorily take account the high monomer exponent as is observed in Fig.1. Deviation of the points from the straight line in the figure as the consequence of high monomer

concentrations is, however, the manifestation of the dominance of first term of the denominator over the other.

Adsorption of AM and TU in MO interlayer space

The adsorption isotherm of Fe(III) ion interaction with montmorillonite exhibit L-type nature, which suggests strong sorbate-sorbent interaction. The maximum saturation corresponds to 0.98 meq/g of the mineral. Most significantly, the redox characteristics of Fe(III) towards TU remains almost unaltered even when Fe(III) ions are adsorbed by the mineral clay montmorillonite. This is evident from the potentiometric titration data of Fe(III) and Fe M by TU solution (Fig. 4). It is thus believed that the same initiating radicals are also involved when Fe(III) ions are trapped between layered spaces of the mineral[3].

Fig.5 shows that the acrylamide molecules readily intercalate from the aqueous solution into the interlayer space of both forms of the mineral, viz., H as well as Fe(III) forms. Both the isotherms are characterized by two plateau regions indicating two-stage intercalation of amide molecules. The first saturation value is nearly 1.25 mmol/g whereas the second one is just nearly double. The bilayer of acrylamide in the internal surface of the mineral seems to play pivotal role in affecting the initiation of polymerization and its mechanism in the layered space as compared to the homogeneous polymerization. In acidic medium, amides may *a priori* accept a proton on either the oxygen or the nitrogen atom. However, both spectroscopic as well as solution studies support the possibility of coming about of the former alternative.[11] Using infrared spectroscopy, Tahoun and Mortland[12] have confirmed that amides predominantly protonate on the oxygen atom in acidic montmorillonite system. In acidic montmorillonite system, hemisalt formation is observed when excess amide is present, i.e., two amide molecules share a proton through a symmetrical hydrogen bond. On the other hand, thiourea is adsorbed in the mineral layer from the aqueous solution giving rise to the isotherm as shown in Fig. 6. The process of removal of water molecules either from the H^+- clay or Fe^{3+} clay to intercalate TU seems almost identical. Unlike acrylamide , the thiourea leads to the monolayer formation only and maximum adsorption capacity is found to be 1.37 mmol/g, which is consistent with that of monolayer of acrylamide.

Polymerization in MO interlayer space

Polymerization mechanism and kinetics both are affected to a great extent due to the occurrence of the reaction in the mineral microenvironment resulting in the significant increase in the molecular weights and intrinsic viscosities of the polymers. Table 2 shows the polymerization data obtained from the reaction under montmorillonite micro-environment. In general, the R_p's are somewhat lower than those obtained in the case of homogeneous polymerization in the absence of any mineral, maintaining the polymer yield (x_L) almost same. The most significant results of loading Fe(III) in the interlayer space of montmorillonite lie in achieving polymers with high molecular weights. The $[\eta]$ value of the polymers formed in the homogeneous conditions ranges between 14-137 $mL.g^{-1}$. In contrast, the $[\eta]$ displayed by polymers formed in the mineral phase is found to vary from 220 to 487 $mL.g^{-1}$ under identical conditions. The M_v as calculated from viscosity data ranged between $(0.68 \times 10^6 - 1.95 \times 10^6$. Unlike homogeneous polymerization, the monomer exponent of R_p remains fixed near 2.3. (Fig. 1, proposed mechanism, however, predicts an exponent of 2.0; the error in experimental data might be due to heterogeneous nature of the reaction mixture[3]). On the other hand, the TU exponent changes from 2 to 1 due to occurrence of the reaction in montmorillonite interlayer space (Fig.2). In order to measure the metal exponent for the reaction in the mineral phase, R_p's were plotted as a function of Fe(III) ion concentration in the montmorillonite gel phase. The slope of the double logarithmic plot was found to be 0.50 at 50°C (Fig. 3). Significant departure from that of homogeneous reaction was also observed in the nature of the above plot. While the linear termination by Fe(III) is prominent in solution phase reaction as is evident from the observed nature of variation of R_p with Fe(III) ion concentration, transfer to Fe(III) is almost controlled in the case of reaction in the layered space. Thus, it is evident that the modification achieved with respect to the kinetics and mechanism of the acrylamide polymerization in the montmorillonite phase stems from a number of factors, viz., (i) instead of collision between a monomer molecule and an initiating radical, a monomer pair is involved in the initiation step (ii) 'cage effect' is prominent in MO phase reaction where the solvent molecules form a potential barrier around the pair of TU radicals to hinder diffusion of

the radicals and favours their recombination (iii) linear termination by Fe(III) is hindered due to location of Fe(III) ions in the interlayer space. Thus, the mechanism of the reaction in the interlayer space of montmorillonite may be shown as follows[3];

Initiation :

$$\overline{Fe(III)} + TU \overset{K}{\rightleftharpoons} \underbrace{\overline{Fe(III)} - TU}_{\text{Complex}} \quad \ldots(11)$$

$$\overline{Fe(III)} - TU + TU \xrightarrow{k_d} \overline{Fe(II)} + (2TU^{\cdot}) + H^+ \quad \ldots(12)$$

$$(TU^{\cdot}) + M_2H^+ \xrightarrow{k_i} M_1 + M + H^+ \quad \ldots(13)$$

Propagation :

$$M_1^{\cdot} + M \xrightarrow{k_p} M_2^{\cdot}$$

$$M_{n-1}^{\cdot} + M \xrightarrow{k_p} M_n^{\cdot} \quad \ldots \quad \ldots\text{etc.} \quad \ldots(14)$$

Termination :

$$M_n^{\cdot} + M_n^{\cdot} \xrightarrow{k_t} M_n - M_n \quad \ldots(15)$$

$$(TU^{\cdot}) + \overline{Fe(III)} \xrightarrow{k_t'} TU + \overline{Fe(II)} \quad \ldots(16)$$

$$(2TU^{\cdot}) \xrightarrow{k_t''} TU - TU \quad \ldots(17)$$

Above scheme of reaction together with psedo-steady state assumption enable one to derive the rate equation as

$$R_p = \frac{k_p(k_d k_i K K'/k_t k_t'')^{1/2} K_{tu}^a (K_m^a)^2 (L_0^a)^3 [\overline{Fe(III)}]^{1/2} [TU]_s [M]_s^2}{(1 + KL_0^a K_{tu}^a [TU]_s)^{1/2}} \quad \ldots(18)$$

(Subscript 's' refers to solution phase and, k =apparent protonation constant of AM in MO interlayer space at a fixed pH (or, a formation constant) ; K_{tu}^a =selectivity co-efficient of TU adsorption onto MO; K_m^a =selectivity coefficient of AM adsorption onto MO; L_0^a =total active sites in unit mass of MO)

where the quantity $KL_0^a K_{tu}^a$ $[TU]_s$ is insignificant compared to unity under present reaction condition and hence can be neglected. The Eq. (18) could satisfactorily explain the behaviour of the Fe(III)-TU initialised acrylamide polymerization exhibited in the aqueous montmorillonite layered space.

Acknowledgement

The authors are thankful to the CSIR., New Delhi, for financial support.

References

1 McCormick C L & Chen G S, *J Polym Sci Polym Chem Ed*, 22 (1984) 3633.
2 Bera P & Saha S K, *Macromol Rapid Commun*, 18(1997) 261.
3 Bera P & Saha S K, *Polymer*, 39(1998) 1461.
4 Jackson M L, *Soil Chemical Analysis* (Prentice Hall of India (P) Ltd., New Delhi), 1973, 168.
5 Francois J, Sarazin D, Schwartz T & Weill G, *Polymer*, 20 (1979) 969.
6 Candau F, Leong Y S, Pouyet G & Candau S, *J Coll Inf Sci*, 101 (1984) 167.
7 Collison E, Dainton F S & McNaughton G S, *Trans Faraday Soc*, 53(1957) 489.
8 Saha S K & Greenslade D J, *Bull Chem Soc Jpn*, 65(1992) 2720.
9 Hsu W C, Kuo J F & Chen C Y, *J Polym Sci Part A Polym Chem*, 31 (1993) 267.
10 Pustelnik N & Soloniewiez, *Chem Anal (Warsaw)*, 21 (1976) 503.
11 Theng B K G, *The Chemistry of Clay-Organic Reactions*, (Adam Hilger, London), 1974, 111.
12 Tahoun S & Mortland M M, *Soil Sci*, 102 (1966) 248.

EUROPEAN POLYMER JOURNAL

Published by Pergamon

An imprint of Elsevier Science Ltd.

Editor-in-Chief
Professor J V Dawkins
Loughborough University
Chemistry Department
Loughborough
Leics LE11 3TU
England
Fax: +44 (0) 1509 223925
E-mail E.PolymerJ@lboro.ac.uk

January 29, 1999

Ref: 196/98

Dr. S.K. Saha,
Department of Chemistry,
University of North Bengal,
Darjeeling - 734430,
INDIA.

Dear Dr. Saha,

I write to follow up my letter dated 6 January 1999 concerning your manuscript entitled:

"Water-Soluble Copolymers of Acrylamide with Diacetone Acrylamide and N-t-Butyl Acrylamide on Aqueous Montmorillonite Surface : Synthesis and Characterisation"

I am pleased to report that this paper is accepted for publication.

Manuscripts, diagrams etc. and proofs are kept in the Editorial Office for a period of one year six months after the above acceptance date. On request we are prepared to return these papers to the author(s) at the end of this period. Thereafter, this material will be destroyed.

Thank you for this contribution to European Polymer Journal.

Could I request that you consider the request on the attached sheet and, if possible, let me have a disk at your earliest convenience.

Yours sincerely,

John Dawkins

Professor J.V. Dawkins

Encs.

Please quote the above reference number in any correspondence

Water-soluble copolymers of acrylamide with diacetone-acrylamide and N-tbutyl acrylamide on aqueous mont-morillonite surface: Synthesis and characterisation.

P. Bera and S.K.Saha
Department of Chemistry
University of North Bengal
Darjeeling-734430, India.

ABSTRACT

The copolymerisation of acrylamide (AM) with N-(1,1-dimethyl-3-oxybutyl) acrylamide (DAAM) and N-t butylacrylamide (N-t BAM) by Fe(III) - thiourea redox initiator has been studied by loading the Fe(III) ions in the interlayer spaces of montmorillonite prior to the polymerisation reaction. The values of $r_1 r_2$ have been determined as 0.43 for the AM : DAAM monomer pair and 0.70 for the AM:N-t BAM pair. The intrinsic viscosities of the copolymers were found to decrease with an increase in the feed composition of DAAM or N-t BAM. The microstructure of copolymers including mean sequence length distribution is predicted for a range of feed compositions through the knowledge of reactivity ratios.

INTRODUCTION

High molecular weight polyacrylamides have found applications as effective flocculants and chemical grouts [1]. Copolymers of acrylamide have shown a number of properties leading to variety of industrial applications including those as water-soluble viscofiers and displacement fluids in enhanced oil recovery [2]. Two of the critical limitations of polyelectrolytes are, however, loss of viscosity in the presence of mono or multivalent electrolytes (viz., NaCl, $CaCl_2$ etc.) and ion binding to the porous reservoir rock substrates. Redox initiated polymerisation is one of the most common method applied in aqueous polymerisation because of simplicity of the technique as well as reasonably high yield and reaction rates. One major difficulty of such a technique is, however, fast termination process via electron transfer to the oxidant of the redox couple. Recently, a novel method has been demonstrated by which the chain growth was enhanced by trapping the metal oxidants in the interlayer space of montmorillonite [3,4]. The later procedure ensures slow termination due to the inability of the growing polymer chain to transfer to the metal oxidant trapped in the layered space.

In the present work, attempts have been made to prepare water soluble copolymers of acrylamide with either N-(1,1-Dimethyl-3-Oxybutyl) acrylamide (commonly referred to as Diacetone acrylamide, DAAM) or N-t butyl acrylamide (N-t BAM) on the montmorillonite surface by interlayer-trapped Fe(III) ions in the presence of thiourea (TU). Importance of the study lie in the fact that (i) the applied technique provides high molecular weight polymer having high intrinsic viscosities and, (ii) atleast one of the above copolymers has already shown some promises by not losing its solution viscosities in the presence of added electrolytes [5]. Characteristics of the copolymers including the reactivity ratios for the respective monomers are determined and the microstructures are predicted.

Experimental Procedures

Materials : Acrylamide (reagent grade, Fluka) was purified by recrystallisation from methanol (two times) and dried in vacuum oven at 45°C for overnight. Thiourea (E.Merck) was used after recrystallisation three times from distilled water (m.p. 180°C). Method of preparation and characteristics of Fe(III)-montmorillonite (FeM) was similar to one as already described [3]. N-(1,1-dimethyl-3-oxybutyl) acrylamide (reagent grade, Fluka) was recrystallised twice from methanol and vacuum dried. N-t butyl acrylamide (reagent grade, Fluka) was used as received.

Polymerisation :

Poly (acrylamide - Co-N-(1,1-Dimethyl-3-oxybutyl) acrylamide

The copolymerisation of AM with DAAM was conducted in aqueous solution at 50°C using 0.5% (W/V) of FeM and 0.04 M of TU couple as initiator. Table-1 lists reaction parameters for four series of reactions in which the ratios of monomers in the feed and reaction times were varied. A specified amount of DAAM dissolved in distilled water was added to the mixture of AM and TU solutions of known concentrations in 100 ml stoppered pyrex bottles under nitrogen. In another set of bottles, known amounts of aqueous FeM suspensions were degassed and, finally added to the former bottles under nitrogen atmosphere. The pH of the final mixture was adjusted at 2.0± 0.1 by dropwise addition of 0.01 M HCl solution, well shaken and immediately placed in thermostatic bath of appropriate temperature. pH adjustment was necessary to ensure the formation of adequate amount of the amido- sulfenyl primary radicals to initiate the copolymerisation reaction [6]. After the designated time interval, the copolymerisation reaction was stopped by diluting the reaction mixture with chilled water, keeping the vessel in the ice-bath and FeM separated by centrifugation (1.5×10^4 r.p.m.). AM-DAAM copolymers was precipitated out by the addition of excess acetone. The copolymers and FeM were washed

separately by acetone and water respectively. The copolymers and FeM were then dried at 60°C under vacuum for 48 hours. Conversions were determined gravimetrically.

Poly (acrylamide-Co-N-tert-butylacrylamide)

Since N-t-butylacrylamide is insoluble in water, the monomer was dissolved in micellar pseudo-phase of nonionic surfactant, Triton-X 100(R). Four series of copolymerisation of acrylamide with N-t-butyl acrylamide with a total monomer concentration of 0.42 M were conducted in aqueous solution at 50°C using 0.50% FeM(w/v) and 0.04M TU as the initiator. Reaction parameters for four series of reactions are given in Table-2. The reaction procedures were the same as those described for the preparation of copolymers of acrylamide with diacetoneacrylamide.

Elemental Analysis

Elemental analyses for carbon and nitrogen of AM-DAAM and AM-N-t BAM copolymers were conducted by RSIC, Chandigarh, India (Table 1,2). The copolymer compositions were calculated based on C/N ratios because of the variability of absolute values due to the hygroscopic nature of the polymers. Elemental analyses were conducted at polymer conversion levels, i.e. low and high, to assess drift in the copolymer composition.

Viscosity Measurements

A series of copolymer solution of different concentrations in aqueous 0.1M NaCl are prepared from the 0.5% stock solution. The time of flow of the solutions and solvent are recorded by Ubbelohde type viscometer placed in thermostatic water bath at 30°C (± 0.2°C) . Specific viscosity (η_{sp}) is calculated from the time of flow data. The intrinsic viscosity (η) value is obtained from the intercept of the plot of η_{sp}/C versus C following the relation,

$[\eta] = \eta_{sp}/C$ Lim C 0 , where C stands for concentration of copolymer solution.

RESULTS AND DISCUSSION

Studies on reactivity ratios : The variation in feed ratios and the resultant copolymer compositions (Table 1 and 2) as determined from elemental analyses were used to calculate the reactivity ratios for the AM-DAAM and AM-N-t BAM copolymer systems. The Fineman - Ross method [7] and Kelen-Tüdos method [8] were employed to determine the monomer reactivity ratios at low conversion polymerisation data. Figure 1 is the Fineman - Ross plot for the copolymer of acrylamide (M_1) and diacetoneacrylamide (M_2). The reactivity ratios r_1 and r_2 for the monomer pair M_1 and M_2 can be determined by

$$F(f-1)/f = r_1(F^2/f) - r_2 \qquad (1)$$

where $f = d(M_1)/d(M_2)$, $F = (M_1)/(M_2)$

The reactivity ratio r_1 was determined to be 0.69 ± 0.03 from the slope and $r_2 = 0.62 \pm 0.05$ from the intercept. However, it is well known that in Fineman-Ross analysis, values of reactivity ratios are dependent on indexing of the monomers. On reversing the indexes of the monomers (i.e., assuming DAAM as M_1 and AM as M_2) the values of reactivity ratios are changed to 6.18 ± 0.17 and 1.06 ± 0.07 for acrylamide and diacetoneacrylamide respectively. Kelen - Tüdos approach was also applied for evaluation of reactivity ratios for the same monomer pair according to

$$\upsilon = r_1\xi - r_2 (1-\xi)/\alpha \qquad (2)$$

where $\upsilon = G/\alpha + H$ and $\xi = H/\alpha + H$.

The transformed variables G and H are given by

$$G = \frac{[M_1]/[M_2]\,[(d[M_1]/d[M_2]) - 1]}{d[M_1]/d[M_2]} \qquad (3)$$

$$H = \frac{([M_1]/[M_2])^2}{d[M_1]/d[M_2]} \qquad (4)$$

The parameter α is calculated by taking square root of the product of the lowest and highest values of H for the copolymerisation series. A plot of the data according to the Kelen-Tüdos method is shown in Figure-2. Reactivity ratios were determined for AM : DAAM monomer pair as $r_1 = 0.71$ and $r_2 = 0.61$ respectively. The observed data in the Kelen-Tüdos plot are linear, an indication that these copolymerisation follow the conventional copolymerisation kinetics under a prerequisite that the reactivity of a polymer radical is only determined by the terminal monomer unit [9]. The values of r_1 and r_2 obtained from Fineman-Ross and Kelen-Tüdos treatments for the copolymerisation of acrylamide with diacetone acrylamide on montmorillonite surface are listed in Table 3.

Reactivity ratio studies were also conducted for the copolymerisation of acrylamide with N-t-butylacrylamide using Fineman-Ross (Figure-3) and Kelen-Tüdos (Figure 4) methods. The calculated reactivity ratios are listed in Table 4. Figure 5 shows the composition as a function of the acrylamide in the feed based on the experimentally determined reactivity ratios in the copolymerisation of AM with DAAM and with N-t BAM. The AM-DAAM copolymers with $r_1 r_2 = 0.43$ and the AM-N-t BAM copolymers with $r_1 r_2 = 0.70$ exhibit an opposite tendency toward alternation. Experimental points on the figure are, however, restricted upto 80 mole % of AM in the feed because no copolymer was formed below that value. Previous study on the copolymerisation of AM with DAAM by potassium persulfate[2] initiator showed a variation of r_1 and r_2 values from 0.76 to 0.83 and 0.92 to 0.99 respectively for the different methods applied. The Kelen-Tüdos analysis which is considered more reliable than others, shows that r_1 values for the copolymerisation of AM with N-t BAM are considerably higher than AM-DAAM copolymers, where as, those of r_2 are smaller in the case of AM-N-t BAM than that of the other copolymer.

Copolymer microstructure

The microstructures of the AM-DAAM and AM-N-t BAM copolymers are expected to be important in determining the solution properties of copolymers. As mentioned earlier, observed data follow the conventional coolymerisation equation and the adherence of the data to this equation is an important point in establishing the validity of the statistical microstructure analyses. The statistical distribution of monomer sequences, M_1 - M_1, M_2 - M_2, and M_1 - M_2 may be calculated utilizing equns. (6-8) [10 - 12].

$$X = \phi - 2\phi_1 (1-\phi_1)/\{1+[(2\phi_1 - 1)^2 + 4r_1r_2\phi_1(1-\phi_1)]\}^{1/2} \quad (6)$$

$$Y = (1-\phi_1) - 2\phi_1 (1-\phi_1)/\{1+[(2\phi_1 - 1)^2 + 4r_1r_2\phi_1(1-\phi_1)]\}^{1/2} \quad (7)$$

$$Z = 4\phi_1 (1-\phi_1)/\{1+[(2\phi_1 - 1)^2 + 4r_1r_2\phi_1(1-\phi_1)]\}^{1/2} \quad (8)$$

The mole fractions of M_1 - M_1, M_2 - M_2, and M_1 - M_2 sequences in the copolymer are designated by X, Y and Z respectively. The copolymer composition is ϕ_1 and, r_1 and r_2 are the reactivity ratios, for the respective monomer pairs. Mean sequence lengths, μ_1 and μ_2, can be calculated utilizing equation (9) and (10) with the consideration of compositional drift (10).

$$\mu_1 = 1 + r_1[M_1]/[M_2] \quad (9)$$

$$\mu_2 = 1 + r_2 [M_2]/[M_1] \quad (10)$$

The intermolecular linkage and mean sequence length distributions for the AM-DAAM and the AM-N-t BAM copolymers are listed in Table 5 and 6 respectively (Kelen-Tüdos values of reactivity ratios were used for the calculations). For the series of AM-DAAM copolymers, the mean sequence length of acrylamide, μ_{AM}, varied from 30.03 at an 96.36/3.64 mol ratio of AM/DAAM in the copolymer to 4.01 with a 78.77/21.23 mol ratio. For those compositions, values of μ_{DAAM} were 1.01 and 1.14 respectively. On the other hand, the

AM-N-t BAM copolymers had μ_{AM} value of 62.50 and 7.37 at 98.33/1.67 and 89.42/ 10.58 mol ratios of AM/N-t-BAM respectively. Above values for $\mu_{N\text{-}t\,BAM}$ were 1.01 and 1.11 respectively.

Effect of Feed Composition

The effect of feed composition on intrinsic viscosity of copolymers synthesized at high conversion was studied for both AM-DAAM and the AM-N-t BAM copolymers listed in Table 1 and 2 respectively. Figure 7 illustrates the effect of feed composition on the intrinsic viscosity for each copolymer series. The observed decrease in intrinsic viscosity with increasing diacetoneacrylamide or N-tert-butylacrylamide co-monomer concentrations may be explained by increased crosstermination rates of copolymerisation as compared to the very low rate of termination observed for acrylamide, resulting in the decrease of the overall molecular weight of the copolymers [13, 14].

ACKNOWLEDGEMENT

Authors are thankful to CSIR, New Delhi for financial support.

REFERENCES

1. P.Molyneux. *Water-Soluble Synthetic Polymers: Up date I and II*, Microphile Associates, U.K. (1988).

2. C.L.McCormick and G.S.Chen. *J.Polym. Sci. Polym. Chem.* **22**, 3633 (1984).

3. P. Bera and S.K.Saha. *Macromol.* Rapid Commun. **18**, 261 (1997)

4. P. Bera and S.K.Saha, *Polymer* **39**, 1461 (1998).

5. C.L.McCormick and G.S.Chen. *J.Polym. Sci. Polym. Chem.* **22**, 3649 (1984).

6. S.K.Saha and D.J.Greenslade. *Bull. Chem. Soc. Jpn.* **65**, 2720 (1992).

7. M. Fineman and S.D.Ross, *J. Polym. Sci.* **5**, 259 (1950).

8. T.Kelen and F. Tüdos. *J. Macromol. Sci. Chem.* **A9**, 1 (1975)

9. S.Iwatsuki, A. Kondo and H. Harashina. *Macromolecules* **17**, 2473 (1984).

10. S.Igarashi, *J. Polym. Sci. Polym. Lett.* **1**, 359 (1963).

11. C.W.Pyun. *J. Polym. Sci.* Part A2. **8**, III (1970).

12. H.J.Harwood, *J. Polym. Sci.* Part C. **25**, 37 (1968)

13. W.M.Thomas, in *Encyclopedia of Polymer Science and Technology*, Vol. I, N. Bikales, Ed. Wiley-Interscience, New York, 177 (1964).

14. F.S.Dainton and M. Tordoff. *Trans. Faraday Soc.* **53**, 666 (1957).

Ligends of figures

Fig. 1 Determination of reactivity ratios for copolymerisation of AM(M_1) with DAAM (M_2) by Fineman-Ross method.

Fig. 2 Kelen-Tüdos plot for the determination of reactivity ratios for copolymerisation of AM with DAAM.

Fig. 3 Determination of reactivity ratios for copolymerisation of AM(M_1) with N-t BAM(M_2) by Fineman-Ross method.

Fig.4 Determination of reactivity ratios for copolymerisation of AM with N-t BAM by Kelen-Tüdos method.

Fig. 5 Copolymer composition as a function of feed composition for the copolymerisation of AM with DAAM (curve 1) and AM with N-t BAM (curve 2).

Fig. 6 Effect of feed composition on the intrinsic viscosity of AM-DAAM(O) and AM-N-t BAM (●) copolymers.

Table - I

Reaction parameters for the copolymerization of AM with DAAM at 50°C in Distilled water (Total Monomer concentration = 0.42 M)

Sample number	Monomer concentration in the feed (M)			Reaction time (min.)	Conversion(%)	Elemental Analysis (wt%)		Mol % DAAM in copolymer	[η] $ml.g^{-1}$
	[AM]	[DAAM]	[AM]/ [DAAM]			C	N -		
DAAM-10-1	0.41	0.01	41	90	37.10	41.46	15.03	3.60 ± 0.04	
DAAM-10-2	0.41	0.01	41	150	48.13	41.72	15.15	3.52 ± 0.04	420
DAAM-10-3	0.41	0.01	41	210	54.19	42.62	14.82	5.91 ± 0.04	
DAAM-20-1	0.40	0.02	20	90	23.37	42.08	14.51	6.32 ± 0.08	
DAAM-20-2	0.40	0.02	20	150	31.84	42.03	14.26	7.32 ± 0.09	350
DAAM-20-3	0.40	0.02	20	210	40.54	43.05	14.81	6.54 ± 0.09	
DAAM-30-1	0.38	0.04	9.5	90	6.00	43.47	13.51	12.52 ± 0.20	
DAAM-30-2	0.38	0.04	9.5	150	15.40	43.30	13.52	12.24 ± 0.20	340
DAAM-30-3	0.38	0.04	9.5	210	30.37	44.31	14.11	11.05 ± 0.20	
DAAM-40-1	0.34	0.08	4.25	90	11.10	45.28	12.36	21.22 ± 0.30	
DAAM-40-2	0.34	0.08	4.25	150	6.47	45.25	11.39	27.23 ± 0.40	333
DAAM-40-3	0.34	0.08	4.25	210	7.41	46.23	12.70	20.71 ± 0.30	

Table - 2

Reaction Parameters for the copolymerisation of AM with N-t BAM At 50°C (Total Monomer Concentration = 0.42 M)

Sample number	Monomer concentration in the feed (M)			Reaction time (min.)	Conversion(%)	Elemental Analysis (wt%)		Mol % N-t BAM in copolymer	[η] ml.g^{-1}
	[AM]	[N-t-BAM]	[AM]/ [N-t BAM]			C	N		
N-t-BAM-10-1	0.41	0.01	41	90	27.01	41.16	14.78	6.21 ± 0.08	
N-t-BAM-10-2	0.41	0.01	41	150	35.81	40.32	15.53	1.66 ± 0.04	430
N-t-BAM-10-3	0.41	0.01	41	210	55.61	42.28	15.50	4.57 ± 0.06	
N-t-BAM-20-1	0.40	0.02	20	90	36.27	40.91	15.62	1.31 ± 0.04	
N-t-BAM-20-2	0.40	0.02	20	150	40.78	40.94	15.08	4.15 ± 0.04	415
N-t-BAM-20-3	0.40	0.02	20	210	52.79	42.02	15.07	6.32 ± 0.08	
N-t-BAM-30-1	0.38	0.04	9.5	90	28.58	42.10	14.21	11.42 ± 0.20	
N-t-BAM-30-2	0.38	0.04	9.5	150	31.81	41.11	14.94	5.21 ± 0.05	403
N-t-BAM-30-3	0.38	0.04	9.5	210	34.53	43.58	12.79	24.33± 0.30	
N-t-BAM-40-1	0.34	0.08	4.25	90	28.38	42.35	14.29	11.44 ± 0.20	
N-t-BAM-40-2	0.34	0.08	4.25	150	39.40	41.96	14.30	10.57 ± 0.20	300
N-t-BAM-40-3	0.34	0.08	4.25	210	40.98	43.67	13.10	22.25 ± 0.30	

Table-3

Reactivity Ratios for copolymerisation of AM(r_1) with DAAM (r_2)

Method	r_1	r_2
Fineman-Ross[a]	0.69±0.03	0.62 ± 0.05
Fineman-Ross[b]	6.18 ±0.17	1.06 ± 0.06
Kelen-Tüdos	0.70 ± 0.08	0.60 ± 0.09

[a]M_1 = AM, M_2 = DAAM ; [b]M_1 = DAAM, M_2 = AM

Table-4

Reactivity Ratios for copolymerisation of AM(r_1) with N-t BAM(r_2)

Method	r_1	r_2
Fineman-Ross[a]	1.50 ± 0.10	0.50 ± 0.04
Fineman-Ross[b]	1.39 ± 0.08	0.75 ± 0.06
Kelen-Tüdos	1.50 ± 0.10	0.46 ± 0.04

[a]M_1=AM, M_2=N-t BAM ; [b]M_1=N-t BAM, M_2=AM

Table-5

Structural Data for the copolymers of AM with DAAM

Sample Number	Composition[a] (mole%)		Blockiness[b] (mole%)		Alternation[b] (mole%)	Mean Sequence length		μ_{AM}/μ_{DAAM}
	AM	DAAM	AM-AM	DAAM-DAAM	AM - DAAM	μ_{AM}	μ_{DAAM}	
DAAM-10-1	96.36	3.64	92.78	0.06	7.16	30.03	1.01	29.58
DAAM-20-1	93.61	6.39	87.41	0.19	12.40	15.16	1.03	14.71
DAAM-30-1	87.44	12.56	75.67	0.79	23.54	7.72	1.06	7.29
DAAM-40-1	78.77	21.23	60.05	2.51	37.43	4.01	1.14	3.51
DAAM-10-2	96.46	3.54	92.97	0.06	6.97	30.03	1.01	29.58
DAAM-20-2	92.69	7.31	85.70	0.32	13.98	15.16	1.03	14.71
DAAM-30-2	87.73	12.27	76.21	0.76	23.03	7.72	1.06	7.29
DAAM--40-2	72.76	27.24	50.00	4.47	45.54	4.01	1.14	3.51
DAAM--10-3	94.08	5.92	88.32	0.16	11.51	30.03	1.01	29.58
DAAM--20-3	93.49	6.51	87.17	0.20	12.62	15.16	1.03	14.71
DAAM-30-3	88.94	11.06	78.48	0.60	20.92	7.72	1.06	7.29
DAAM-40-3	79.22	20.78	60.83	2.40	36.77	4.01	1.14	3.51

[a] Calculated from elemental analysis ; [b] Statistically calculated from the reactivity ratios.

Table-6

Structural Data for the copolymers of AM with N-t BAM

Sample Number	Composition[a] (mole%)		Blockiness[b] (mole%)		Alternation[b] (mole%)	Mean Sequence length		$\mu_{AM}/\mu_{N\text{-}t\,BAM}$
	AM	N-t BAM	AM-AM	N-t BAM-N-t BAM	AM - N-t BAM	μ_{AM}	$\mu_{N\text{-}t\,BAM}$	
N-t-BAM-10-1	93.78	6.22	87.84	0.28	11.87	62.50	1.01	61.80
N-t-BAM-20-1	98.61	1.39	97.23	0.01	2.75	31.00	1.02	30.30
N-t-BAM-30-1	88.59	11.41	78.16	0.98	20.86	15.25	1.05	14.52
N-t-BAM-10-1	88.56	11.44	78.10	0.98	20.91	7.37	1.11	6.64
N-t-BAM-10-2	98.33	1.67	96.68	0.01	3.30	62.50	1.01	61.80
N-t-BAM-20-2	95.82	4.18	91.77	0.12	8.11	31.00	1.02	30.30
N-t-BAM-30-2	94.75	5.25	89.70	0.20	10.10	15.25	1.05	14.52
N-t-BAM-40-2	89.42	10.58	79.68	0.84	19.48	7.37	1.11	6.64
N-t-BAM-10-3	95.44	4.56	91.03	0.46	8.82	62.50	1.01	61.80
N-t-BAM-20-3	93.68	6.32	87.65	0.29	12.06	31.00	1.02	30.30
N-t-BAM-30-3	75.62	24.38	56.05	4.80	39.14	15.25	1.05	14.52
N-t-BAM--40-3	77.77	22.23	3.95	3.95	36.55	7.37	1.11	6.64

[a]Calculated from Elemental Analysis

[b]Statistically calculated from Reactivity Ratios.

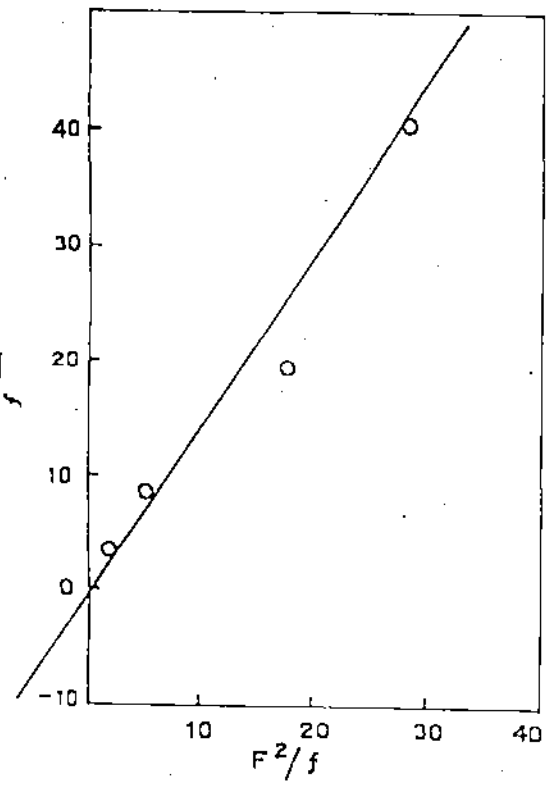

Fig. 3

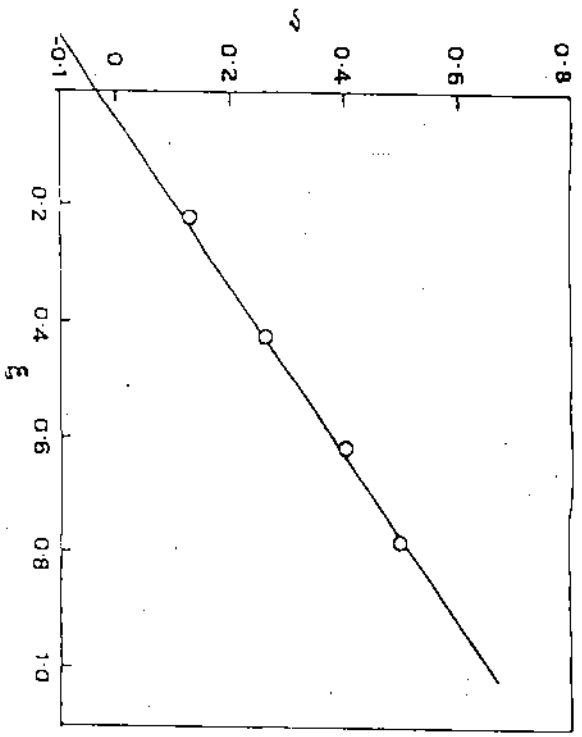

Fig. 2.

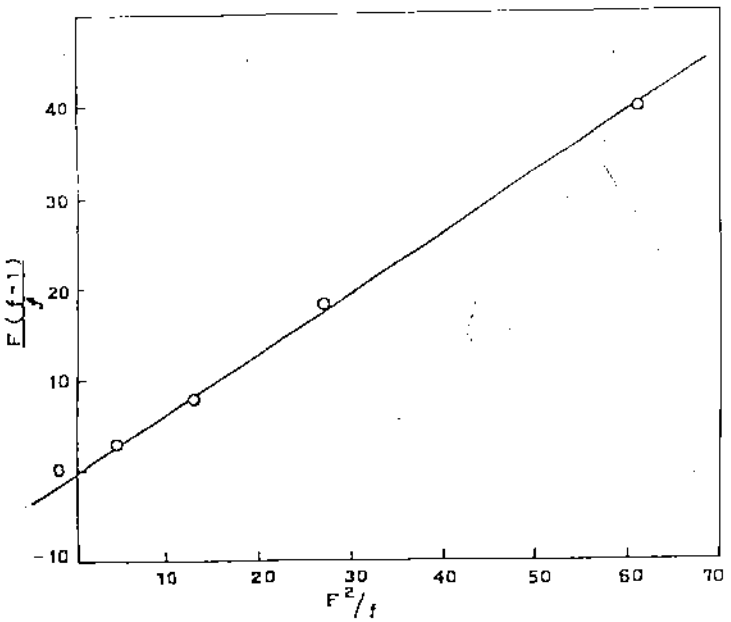

Fig. 1.

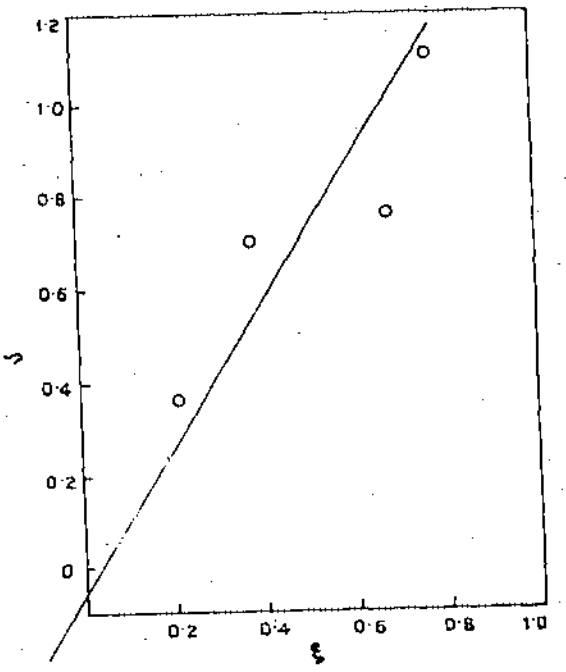

Fig. 4

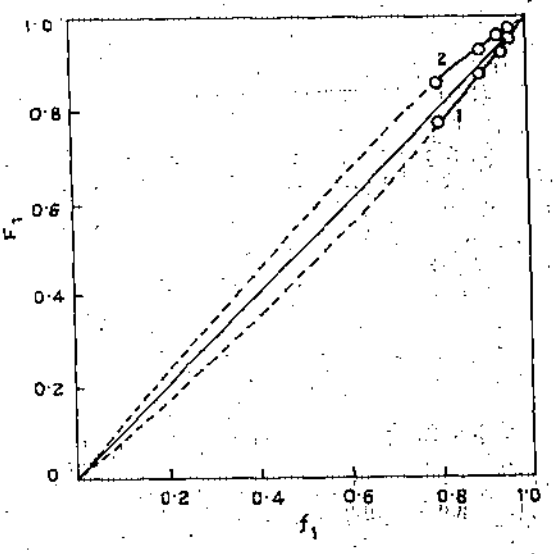

Fig. 5

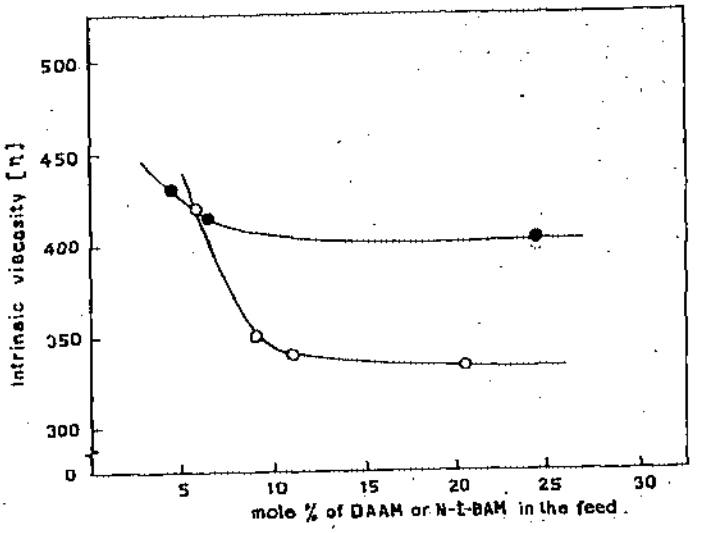

Fig. 6